Barron, J., Larsen, B., et al., 1991
Proceedings of the Ocean Drilling Program, Scientific Results, Vol. 119

47. THE CRETACEOUS/TERTIARY BOUNDARY AT SITE 738, SOUTHERN KERGUELEN PLATEAU[1]

Hans R. Thierstein,[2] Frank Asaro,[3] Werner U. Ehrmann,[4] Brian Huber,[5] Helen Michel,[3] Hideo Sakai,[6] and Birger Schmitz[7]

ABSTRACT

High-resolution stratigraphic evidence of an apparently complete carbonate-rich Cretaceous/Tertiary boundary interval in Section 119-738C-20R-5 from the southern Kerguelen Plateau is summarized and interpreted. The change of the calcareous nannoflora and of the planktonic foraminifers is spread over a laminated interval of about 15 cm thickness. The base of this laminated interval lies in uppermost Maestrichtian chalks, 2 cm below a distinct 2-mm-thick "gray clay" layer, which shows the highest iridium enrichment (18 ppb) measured in this section. No shocked quartz or microspherules, characteristic of an impact, were found. No change in the clay mineralogy, which could be expected for a large volcanic or impact event, could be identified. Elevated metal and iridium concentrations (>1.6 ppb) occur already in the bioturbated uppermost Maestrichtian chalks several centimeters below the "gray clay" and decrease above the iridium peak gradually over a laminated 12-cm-thick interval to background values of 0.1–0.3 ppb Ir. Application of bio- and magnetochronology shows that the accumulation rates of carbonates and clays, but not of the metals, decreased dramatically at the Cretaceous/Tertiary boundary and thus, the lack of dilution may have led to the observed metal concentrations.

LITHOSTRATIGRAPHY

A Cretaceous/Tertiary boundary sequence was recovered at 377.16 m below seafloor (mbsf) in Section 119-738C-20R-5 on the southern Kerguelen Plateau (62.7°S, 82.8°E). Site 738 was drilled in 2252.5 m of water. The Upper Cretaceous sediments consist of indurated white chalks with interlayered cherts and are overlain by softer Paleocene chalks and oozes. A description of Site 738 is found in the *Initial Reports* (Shipboard Scientific Party, 1989).

The Cretaceous/Tertiary boundary found in Section 119-738C-20R-5 appears to be unique because it lies within a clay-rich interval, which in its lowermost 15 centimeters (119-738C-20R-5, 83–98 cm) is finely laminated (Fig. 1). About 2 cm above the base of the laminated interval, a distinct 2-mm-thick gray clay layer at Section 119-738C-20R-5, 96.0–96.2 cm, (377.16 mbsf) was found, hereafter referred to as the "gray clay". This was the second of three apparently complete Cretaceous/Tertiary boundary sections recovered from southern high latitudes, the other being at Site 690 (Maud Rise; Barker, Kennett, et al., 1988) and Site 752 (Broken Ridge; Peirce, Weissel, et al., 1989).

The lithostratigraphic sequence in Section 119-738C-20R-5 is as follows (from bottom up):

117–103 cm: black to dark-gray hard chert with embedded pebbles (3–8 mm across) of porcellanite.

102–98 cm: white, bioturbated limestone grading upward into:

98–96.2 cm: white, indurated chalk with anastomosing light-green <1-mm thick clay laminae.

96.2–96.0 cm: distinct dark-gray, silty clay layer with sharp lower and upper limits.

96.0–82.5 cm: semi-indurated sequence of finely laminated (<1–2 mm thick) white and light-green layers, of more or less constant thicknesses of the laminae across the core in the lower part of the interval (96–90 cm) and with changing thicknesses of individual laminae in the upper part (90–83 cm). Several normal microfaults occur throughout the laminated interval. Irregular upper contact to:

82.5–80.5 cm: semi-indurated, light-brown to white, slightly disturbed chalk and drilling breccia, chalk apparently bioturbated.

80.5 cm to top of core: light-green, semi-indurated chalk with numerous, darker burrows *(Zoophycos, Planolites*, and *Chondrites).*

SAMPLING STRATEGY

When it was realized on board that a reasonably complete Cretaceous/Tertiary boundary interval may have been recovered, Section 119-738C-20R-5 was sampled only with toothpicks for lithologic descriptions and to determine more precisely the nannofossil-paleontological succession. During this initial sampling it was discovered that the margins of the core, and some lighter laminae within the boundary interval (e.g., at Section 119-738C-20R-5, 95.6 cm), contained small numbers of evolved lower Paleocene nannofossils, which were not found in the adjacent green or white laminae if the samples were taken from the central parts of the core. This suggested that fluidized sediment may have been squeezed along the core liner and sporadically into the core along cracks and fractures within the sediment. An X-ray radiograph taken aboard ship shows that the lithified portions of the core are heavily fractured (Fig. 2). These fractures are filled with soft, probably displaced sediment. The laminated interval immediately below and above the boundary clay is undisturbed and depositional, as indicated by the presence of synsedimentary microstructures, such as short, small faults and small, angular disconformities.

A limited number of samples were taken during the cruise above and below the laminated interval. Several months later,

[1] Barron, J., Larsen, B., et al., 1991. *Proc. ODP, Sci. Results*, 119: College Station, TX (Ocean Drilling Program).

[2] Geological Institute, ETH-Zentrum, CH-8092 Zürich, Switzerland.

[3] Lawrence Berkeley Laboratory, University of California, Berkeley, CA 94720, U.S.A.

[4] Alfred Wegener Institute for Polar and Marine Research, Bremerhaven, Federal Republic of Germany.

[5] Smithsonian Institution, Washington, DC 20560, U.S.A.

[6] Tojama University, Gofuku 3190, Toyama City 930, Japan.

[7] Department of Marine Geology, University of Gothenburg, S-402 32 Gothenburg, Sweden.

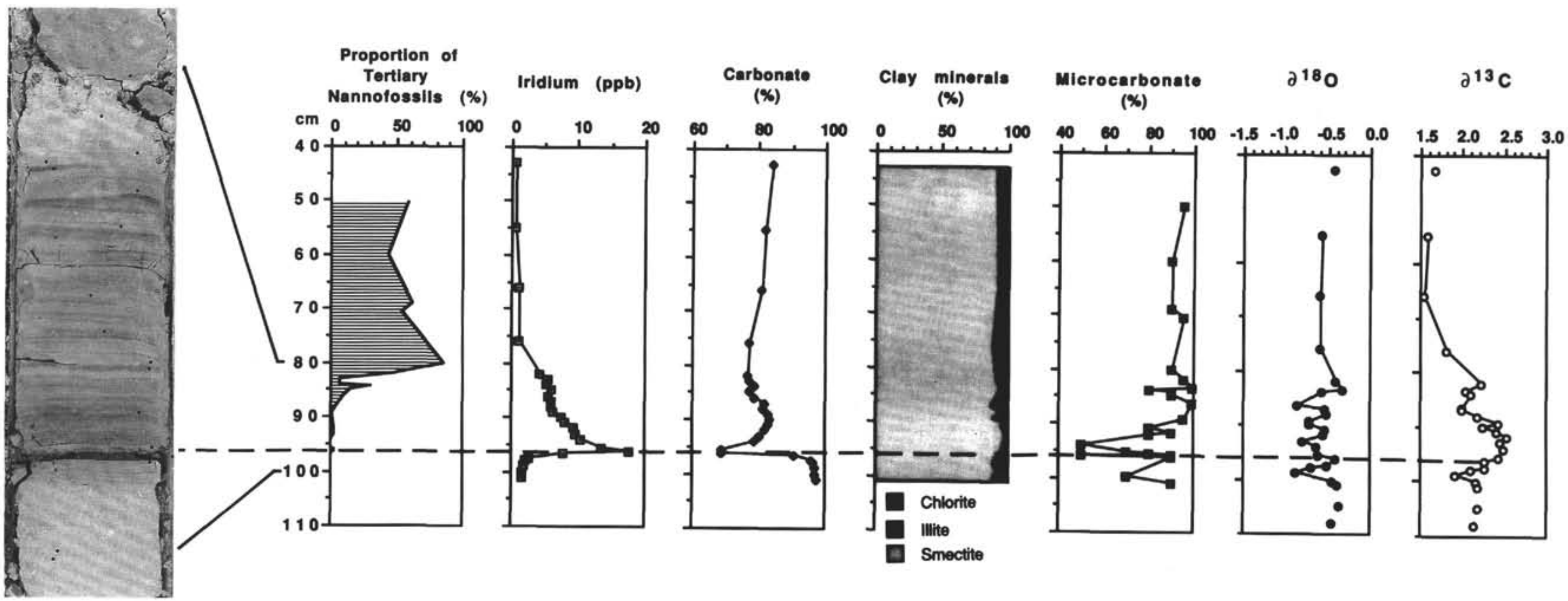

Figure 1. Lithology, precise sampling locations for nannofossil counts (black dots), and microcarbonate estimates and relevant analytical results of the laminated interval around the Cretaceous/Tertiary boundary "gray clay" layer (at Section 119-738C-20-5, 96.0–96.2 cm) from the southern Kerguelen Plateau. Data from Table 1. For further details see text.

Figure 2. X-ray radiograph of the Cretaceous/Tertiary boundary interval (centimeter scale starts at Section 119-738C-20-5, 70 cm) showing the intact laminated sediment fabric between Section 119-738C-20-5, 82 and 97 cm, and fragmentation and disturbance by drilling of more lithified chalk intervals above and below.

after the collaboration of additional specialists had been secured and their sample requirements verified, Section 119-738C-20R-5 was sampled continuously (1.25 cm^3 every centimeter) between 82 and 102 cm and about every 10 cm above to the top of Section 119-738C-20R-5.

Counts of calcareous nannofossil are based on the smear slides made from individual laminae during the cruise, which were compared in a few crucial intervals to the nannofossil assemblages contained in the <38-μm fractions of the subsequent sample set. All other analyses (carbonate content, clay mineral analyses, geochemistry, and foraminifer analyses) were made using the samples taken post-cruise. Those samples represent homogenized 1-cm-thick stratigraphic intervals, with the exception of the 2-mm-thick "gray clay," which was processed separately. The most important analytical data discussed in this article are listed in Table 1. Additional information on the Cretaceous/Tertiary boundary interval can be found in other articles in this volume by Schmitz et al., Huber, Sakai, Wei and Thierstein, and Wei and Pospichal.

CHRONOLOGY AND SEDIMENT ACCUMULATION RATES

The biostratigraphic and magnetostratigraphic data available are documented in detail in this volume in papers by Huber, Wei and Thierstein, and Sakai. Because of coring disturbance, poor core recovery, and equipment problems on board, the original paleomagnetic data were discarded and new measurements on discrete samples were used, although this information is spotty. The magnetostratigraphy, the bioevents, their stratigraphic position, and their assumed ages are summarized in Figure 3 and were arrived at in the following way.

The first occurrence (FO) of *Nephrolithus frequens* has been correlated with the middle part of Subchron 30N at Deep Sea Drilling Project (DSDP) Holes 525A and 527 (Manivit, 1984; Chave, 1984), which corresponds to an age of 67.5 Ma using the paleomagnetic calibration of Berggren et al. (1985). The FO of the planktonic foraminiferal marker *Abathomphalus mayaroensis* is observed in the lowermost sample above a poorly recovered interval of Core 119-738C-21R. The depth of its first appearance level cannot, therefore, be determined with sufficient precision.

The Cretaceous/Tertiary boundary is characterized by a gradual replacement of typical Late Cretaceous nannofossils by typical Tertiary taxa over an interval of several tens of centimeters. Figure 1 shows the percent Tertiary taxa of all nannofossils encountered. The exact placement of the Cretaceous/Tertiary boundary proper at the level of the "gray clay" (Section 119-738C-20R-5, 96.1 cm) is based on the maximum iridium concentration observed there. The age of the Cretaceous/Tertiary boundary was calibrated by Berggren et al. (1985) as 66.4 Ma and the base of Subchron 29N as 66.17 Ma. Based on analyses of orbitally driven bedding cycles within Subchron 29R, Herbert and D'Hondt (1990) placed the Cretaceous/Tertiary boundary 220,000 yr below the top of Subchron 29R and 350,000 yr above the base of Subchron 29R. Using this estimate and the magnetic reversal calibration of Berggren et al. (1985), an age estimate for the Cretaceous/Tertiary boundary of 66.39 Ma results. The first appearance of the planktonic foraminifer *Subbotina pseudobulloides* was correlated with Subchron 29R at DSDP Site 516 (Pujol, 1983; Hamilton and Susyumov, 1983) and in the Bottaccione and Contessa sections near Gubbio (Roggenthen and Napoleone, 1977; Lowrie et al., 1982). In those three sequences FO *S. pseudobulloides* occurs about one-third up from the Cretaceous/Tertiary boundary in the Tertiary part of Subchron 29R, and thus has an estimated age of 66.32 Ma. The nannofossil event FO *Cruciplacolithus tenuis* is correlated with a level two-thirds up the Tertiary part of Subchron 29R in the Bottaccione section (Monechi and Thierstein, 1985) and at DSDP Holes

Table 1. Analytical data of the sediments at and around the Cretaceous/Tertiary boundary at Hole 738C.

Sample	Depth (mbsf)	$\delta^{18}O$	$\delta^{13}C$	Iridium (ppb)	Smectite (%)	Illite (%)	Chlorite (%)	Carbonate (%)	Microcarbonate (%)	Tertiary nannofossils (%)
119-738C-20R-5										
43.0 cm	376.630			0.39	90.5	6.1	2.5	83.7		
50.0 cm	376.700								95	59
55.0 cm	376.750	−0.58	1.57	0.52	92.6	5.4	1.6	82.0		
60.0 cm	376.800								90	43
66.0 cm	376.860	−0.59	1.54	0.92	92.6	6.3	1.0	81.0		
69.0 cm	376.890								90	62
70.5 cm	376.905								95	54
76.0 cm	376.960	−0.59	1.80	1.03	88.1	7.4	4.4	77.0		
80.2 cm	377.002								90	85
82.0 cm	377.020	−0.41	2.22	4.24	90.4	8.4	0.8	76.8	95	46
83.5 cm	377.035	−0.33	2.04	5.54	93.7	4.1	1.0	77.2	99	7
84.0 cm	377.040	−0.57	2.10	5.10	93.2	4.1	1.9	78.5	80	7
84.1 cm	377.041								90	30
85.0 cm	377.050			6.02	91.9	6.2	1.0	76.9	90	15
86.5 cm	377.065	−0.86	1.99	5.50	88.0	10.6	0.7	78.5	99	9
87.0 cm	377.070	−0.53	2.00	6.05	87.0	12.1	0.6	81.7		
88.0 cm	377.080	−0.52	2.17	5.95	94.4	4.8	0.5	81.1		
89.4 cm	377.094	−0.71	2.43	6.17	88.8	9.9	0.8	83.0	95	1
90.0 cm	377.100	−0.72	2.25	7.53	96.0	3.1	0.5	83.5		
91.0 cm	377.110	−0.53	2.40	8.05	94.2	4.9	0.6	83.0	80	1
92.0 cm	377.120	−0.56	2.53	9.33	97.5	1.9	0.2	81.9	90	2
92.3 cm	377.123								80	2
93.0 cm	377.130	−0.79	2.44	9.67	97.3	2.0	0.5	80.1		
94.2 cm	377.142	−0.63	2.50	10.45	96.2	3.2	0.3	78.7	50	0
95.3 cm	377.153								70	0
95.7 cm	377.157	−0.62	2.43	13.54	94.7	3.4	1.1	68.6	80	0
95.9 cm	377.159								90	2
96.1 cm	377.161			17.76	91.0	8.2	0.3	69.0	50	2
96.4 cm	377.164	−0.41	2.25	7.71	91.0	6.8	1.9	90.7	90	0
97.5 cm	377.175	−0.52	2.27	2.54	88.2	7.5	3.8	96.0		
98.0 cm	377.180	−0.70	2.09	2.13	88.5	6.5	3.3	96.3		0
99.0 cm	377.190	−0.88	1.90	1.79	93.7	4.5	1.1	96.9		
99.8 cm	377.198								70	0
100.3 cm	377.203	−0.45	2.16	1.64	88.1	8.6	2.9	97.0		
101.0 cm	377.210	−0.39	2.17	1.65	88.5	8.3	3.0	97.2	90	0
119-738C-20R-4										
130.0 cm	376.000	−0.44	1.67							
119-738C-20R-CC										
	379.900	−0.38	2.18							
119-738C-21R-CC										
	389.600	−0.46	2.13							

Note: The Cretaceous/Tertiary boundary clay is at Section 119-738C-20R-5, 96.0–96.2 cm. The samples for the nannofossil counts and microcarbonate estimates were taken at specific millimeter intervals. The samples for carbonate, clay mineralogical, and geochemical analyses were homogenized over 1-cm intervals and are listed at the corresponding centimeter levels.

525A and 527 (Manivit and Feinberg, 1984), where FO *Cruciplacolithus edwardsii* was used, which we consider to be a junior synonym of *C. tenuis*. In other sections FO *C. tenuis* has been correlated to the lower part of Subchron 29N, such as in the Contessa section (Monechi and Thierstein, 1985) and at DSDP Site 577 (Monechi et al., 1985). As all samples at Hole 738C between the "gray clay" and FO *C. tenuis* and FO *S. pseudobulloides* are reversely magnetized (Sakai, this volume), both of these events must occur within Subchron 29R. The fact that FO *S. pseudobulloides* occurs above FO *C. tenuis* but still within Subchron 29R suggests that the former may be time-transgressive with a younger age in high latitudes than in low latitudes. Assuming an earliest appearance level of *C. tenuis* as observed in the Bottaccione section and at DSDP Holes 525A and 527, an age calibration of 66.24 Ma for FO *C. tenuis* results. The age estimates for FO *Chiasmolithus danicus* and FO *Fasciculithus tympaniformis* are from Berggren et al. (1985). FO *C. danicus* has been correlated to the upper part of Subchron 29N and FO *F. tympaniformis* to Subchron 26R in numerous sections (Monechi and Thierstein, 1985).

The paleomagnetic data confirm that the Cretaceous/Tertiary boundary at Site 738 lies in a reversely magnetized interval, corresponding to Subchron 29R. The paucity of paleomagnetic data in the adjacent cores prevents any closer interpretation of the magnetochronology. We therefore are restricted to the biostratigraphic events for estimates of sedimentation rates.

Assuming a slow and continuous sedimentation of the entire Cretaceous/Tertiary boundary interval and using the age calibrations discussed previously, average sedimentation rates for the intervals between the biostratigraphic events can be calculated (Fig. 3). For the 32 m of uppermost Maestrichtian chalks an average sedimentation rate of 2.88 cm/Ka (1 Ka = 1000 yr) results. A drop in sedimentation rate to about 0.2 cm/Ka for the lowermost 25 cm above the "gray clay" is calculated with a gradual recovery to an average sedimentation rate of 0.9 cm/Ka in the lower half of the lower Danian (next 12.6 m, representing

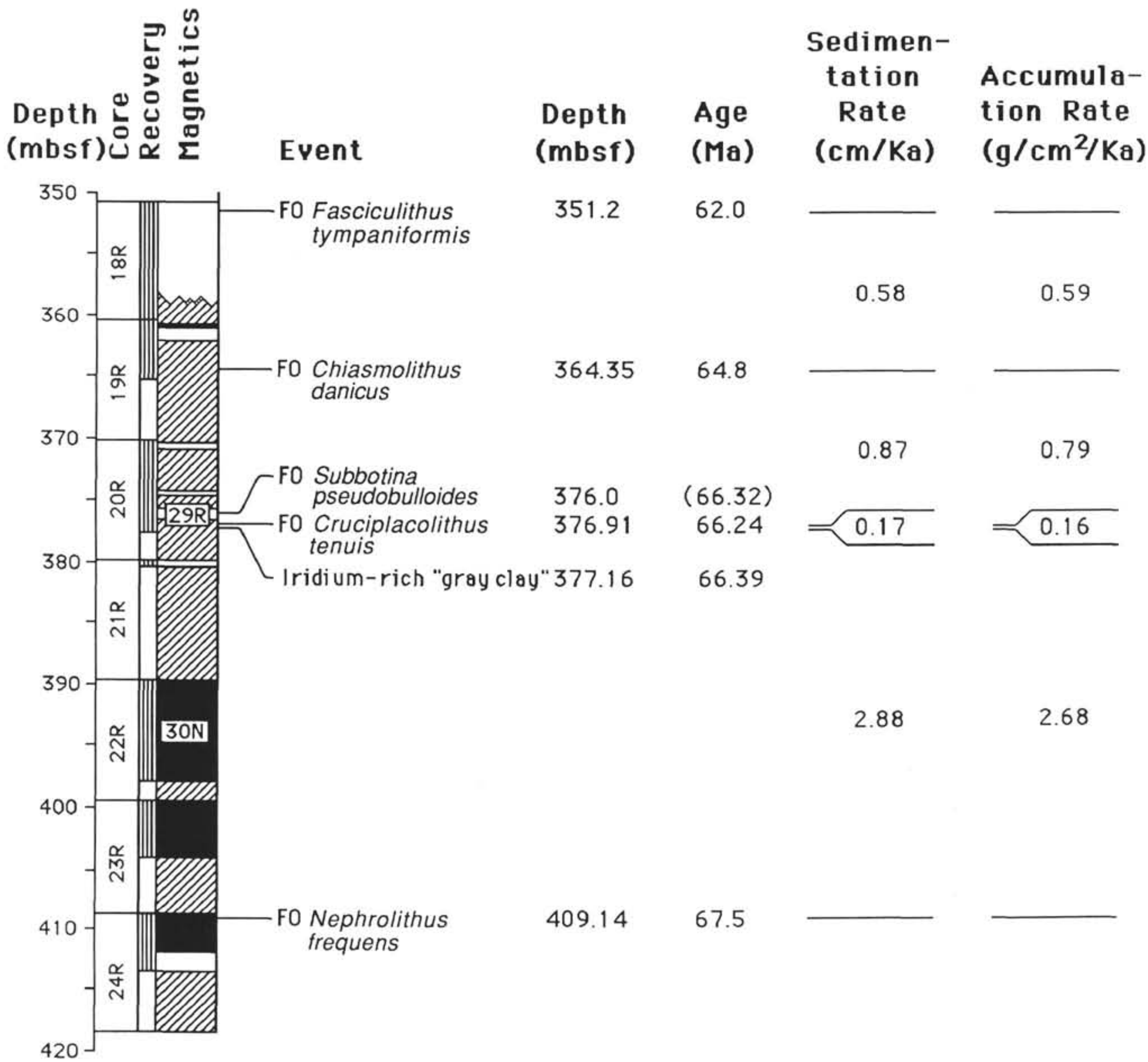

Figure 3. Recovery, magnetostratigraphy, biochronology, and sedimentation and accumulation rates of the Cretaceous/Tertiary boundary interval of Hole 738C. For details see text.

1.44 m.y.), followed by an average sedimentation rate of 0.6 cm/Ka in the upper half of the lower Danian (13.15 m representing 2.8 m.y.).

Assuming continuous sedimentation and using the available porosities and dry-bulk densities (Barron, Larsen, et al., 1989, p. 266), average accumulation rates can be calculated for the same intervals. The results indicate that on the Kerguelen Plateau the relatively high average latest Cretaceous accumulation rate of 2.7 g/cm^2/Ka decreased dramatically (by a factor of 17) to 0.16 g/cm^2/Ka during the earliest 150,000 yr following the deposition of the "gray clay" layer. Subsequently, a partial recovery to accumulation rates about one-quarter of the Late Cretaceous values is observed (Fig. 3).

We have also considered the possibility that the laminated interval at Site 738 was deposited very rapidly and might represent the record of repeated passages of tidal waves which could have been generated by an oceanic impact. The lithologic succession at Site 738 could thus be interpreted in the following way. Pelagic sedimentation of the upper Maestrichtian chalks up to the base of the gray clay layer (Section 119-738C-20R-5, 96.2 cm) would have been interrupted by an impact-related tsunami event. This event could have disturbed the top few centimeters of unconsolidated uppermost Maestrichtian sediments leading to the elimination of any burrowing features. Subsequently, the gray clay and the 14-cm-thick laminated interval above it would have been deposited rapidly under the temporary exclusion of a benthic fauna. The drop in accumulation rates from the uppermost Maestrichtian to the lowermost Danian chalks would be even more dramatic. Such a scenario could receive support from a mineralogical or geochemical signature characteristic of impact-related fallout. Since the available data, such as the presence of abundant benthic foraminiferal casts in the "gray clay" layer as discussed below, do not uniquely favor such an interpretation, we have not further considered this interpretation.

CLAY MINERALOGY AND CARBONATE CONTENTS

Methods

The carbonate contents of the bulk sediment were determined by the weight-difference method before and after 10% acetic acid dissolution of the carbonates at the ETH-Zürich. Reproducibility of duplicate carbonate determinations was better than 0.5% $CaCO_3$. The percentage microcarbonate shown in Figure 1 refers to the proportion of recrystallized micritic carbonate particles among other particles, as estimated in the light microscope. The clay mineral composition was analyzed by X-ray diffraction (XRD) of the carbonate-free, <2-μm fraction, which had been isolated by decantation (settling time based on Stokes' law). The available sample sizes were very small (3 to 22 mg of <2-μm fraction); therefore, the samples had to be fixed as texturally oriented aggregates on aluminum sample holders (for details see Ehrmann, this volume). The samples were solvated with 60°C ethylene-glycol vapor for about 12 hr immediately before the analyses.

The XRD measurements were performed with the equipment of the Alfred Wegener Institute: an automated powder diffractometer system, PW 1700 (Philips), with CoKα radiation (40 kV, 40 mA), graphite monochromator, automatic divergence slit, and an automatic sample changer. The samples were X-rayed from 2° to 78° 2θ with an exposure time of 2 s for each step size of 0.02° 2θ.

The clay minerals were identified by their basal reflections. Semiquantitative determinations of the assemblages included empirically estimated correction factors on integrated peak areas of the individual clay mineral reflections (Biscaye, 1964, 1965; Lange, 1982; Reynolds, 1980). The reproducibility is about $\pm$ 2%; values <1% should be regarded as trace amounts. By comparing the observed diffraction patterns with theoretical patterns (Reynolds and Hower, 1970; Reynolds, 1980), the ordering characteristics and composition of the mixed-layer clay minerals could be determined.

Samples were analyzed from the gray clay itself and at 1-cm distances from 6 cm below to 14 cm above it (Table 1 and Fig. 1). Additional wider spaced samples were also processed but did not reveal long-term variations in the clay mineralogy (Ehrmann, this volume).

Results and Discussion

The clay mineralogical analyses of the Cretaceous/Tertiary boundary interval was done to provide information on the changes and sources of the detrital fraction. According to the impact theory, the boundary clay should contain a mixture of detrital, volcanic, and impact-derived material, all well mixed by the impact process (Alvarez et al., 1980). Therefore, a relatively homogenous composition of the layer with only minor spatial variations could be expected. The mineralogy of such an impact-derived clay should be different from that of the locally derived sediments above and below the boundary. Thus, Kastner et al. (1984) found that the boundary clay at Stevns Klint consists of a pure smectite derived from alteration of impact glass, whereas the clay fraction above and below the boundary consists of illite and mixed-layer smectite-illite of detrital origin. In contrast, Elliott et al. (1989) concluded that the boundary clay at Stevns Klint originated in large part from altered volcanic ash. Rampino and Reynolds (1983) and Johnsson and Reynolds (1986) found at several localities that the clay mineralogical composition of the boundary layer is by no means exotic but is essentially the same as above and below the boundary.

The clay mineralogy of the gray clay and of the sediments above and below it is summarized in Table 1. All clay fractions analyzed (<2 μm, carbonate-free) are dominated by smectite. Its proportion ranges from 88% to 97.5%. Illite concentrations range from 2% to 12%, and chlorite concentrations from traces to 4% in all samples. Additionally, some mixed-layer smectite-illite minerals occur, which are randomly interstratified and have a relatively high proportion of illite (60%–70%). Kaolinite was detected consistently in trace amounts of <2% (Ehrmann, this volume). Quartz and feldspar are present in traces in the <2-μm fraction of all samples.

The clay mineral proportions in the "gray clay" are almost identical those of the sediments above and below (Fig. 1), which show very little variability of the locally derived detritus (see also Ehrmann, this volume). However, the clay mineralogy of the Cretaceous/Tertiary boundary at Site 738 differs slightly from other known Cretaceous/Tertiary boundary localities by the presence of small amounts of chlorite and traces of kaolinite and by the composition of the mixed-layer smectite-illites (see Rampino and Reynolds, 1983; Johnsson and Reynolds, 1986; Elliott et al., 1989).

Because there is no significant qualitative or quantitative difference in the clay mineral composition between the "gray clay," the Cretaceous/Tertiary boundary interval and the sediments above and below, it is unlikely that any significant portion of the clayey interval originated from impact-derived or impact-distributed material. The main clay minerals, smectite, illite, chlorite, and kaolinite, occur in about the same proportions, and the mixed-layer smectite-illites have an almost identical composition. However, small proportions of exotic clay minerals could remain undetected by the XRD method. It is most likely that the clay fraction is derived from a local source, which also explains the difference in its clay mineralogy from other Cretaceous/Tertiary boundary localities investigated so far.

The high bulk carbonate contents of the uppermost Maestrichtian sediments (more than 96%) decrease slightly (91%) in the laminated, clayey interval of a few centimeters in thickness immediately below the "gray clay" (Fig. 1). The "gray clay" (Section 119-738C-20R-5, 96.0–96.2 cm) itself and the sample immediately above (119-738C-20R-5, 95–96 cm) show the lowest carbonate contents (69%) within the analyzed interval. Above that level the carbonate contents fluctuate between 77% and 84%. Accumulation of calcium carbonate dropped from about 2.57 $g/cm^2/Ka$ in the latest Maestrichtian chalks to 0.13 $g/cm^2/Ka$ in the lowermost Danian (377.16–376.91 mbsf) and increases in the lower part of the lower Danian to 0.7 $g/cm^2/Ka$ (376.9–364.35 mbsf). The corresponding noncarbonate accumulation rates dropped from a latest Maestrichtian average of 0.11 $g/cm^2/Ka$ to 0.03 $g/cm^2/Ka$ in the lowermost Danian (377.16–376.91 mbsf)(i.e., by a factor of about 4) and increase subsequently to 0.08 $g/cm^2/Ka$, somewhat less than in the uppermost Cretaceous.

IRIDIUM STRATIGRAPHY

Results

Among the results of the neutron activation analyses of a large number of elements performed by Schmitz et al. (this volume) in sediments spanning the Cretaceous/Tertiary boundary, we have reproduced in Figure 1 the distribution of iridium concentrations in the bulk sediment. The highest iridium enrichment (in ppb of the whole rock) of 18 ppb Ir is observed in the "gray clay" (Sample 119-738C-20R-5, 96.0–96.2 cm). The lowest iridium value measured at this site is 0.1 ppb Ir in Sample 119-738C-20R-4, 129 cm (i.e., 117 cm above the "gray clay"; Schmitz et al., this volume). Iridium concentrations in the bioturbated uppermost Cretaceous chalks 5–6 cm below the "gray clay" reach values of 1.6–1.7 ppb Ir and must be considered strongly enriched compared to the values about 1 m higher. The highest iridium concentration in the "gray clay" thus represents an enrichment factor of about 4 compared to latest Cretaceous values and of more than 100 compared to the subsequent Danian background values[8]. The total iridium flux of 320 nanograms (ng) Ir/cm^2 at this site is one of the highest measured to date for any Cretaceous/Tertiary boundary interval. Following the reasoning by Schmitz et al. (this volume), the iridium enrichments in this Cretaceous/Tertiary boundary section are likely of extraterrestrial origin, based on the occurrence of extraterrestrial iridium enrichments in continental Cretaceous/Tertiary boundary sections (Izett and Bohor, 1987; Schmitz, 1988). There are, however, two possible interpretations of the way this extraterrestrial iridium reached the sediments at Site 738 (Schmitz et al., this volume). One interpretation, favored by B. Schmitz, assumes recycling of the iridium through the terrestrial exogenic cycle and deposition with dominantly locally derived clays. Alternatively, F. Asaro and H. V. Michel deduce a direct impact-ejecta fallout based on a normalizing procedure for tantalum, which they consider to be characteristic of terrestrial background clay sedimentation (for further details see Schmitz et al., this volume).

Iridium Accumulation Rates

The sources for the iridium observed in deep-sea sediments and the processes of its precipitation remain enigmatic. Kyte and Wasson (1986) inferred that on the average about 75% of the iridium in slowly accumulating red clays was of extraterrestrial origin, but that sporadically up to about one-half might accumulate by undisclosed authigenic processes. Schmitz et al. (1988) and Dyer et al. (1989) have pointed out the possible important role in noble and transition metal accumulation that microorganisms and changes in the preburial or postburial redox conditions may play. Microbially mediated diagenetic migration is a possible explanation for the increase of the iridium concentrations in the bioturbated uppermost Maestrichtian chalks several centimeters below the "gray clay" layer. Evidence for such diagenetic mobilization has been found around an impact-ejecta horizon in a Precambrian shale sequence (Wallace et al., 1990).

If the average bulk-accumulation rates for the individual chronologic units (Fig. 3) are taken as representative and the iridium is considered to have been deposited contemporaneously with the other sediment particles, then the following history of iridium accumulation can be determined. In the uppermost Maestrichtian bioturbated sediments, 2–5 cm below the "gray clay," iridium was deposited at a rate of 4.5 ng $Ir/cm^2/Ka$ and in the non-bioturbated sediments in the 2 cm immediately below the "gray clay" at a rate of 11.1 ng $Ir/cm^2/Ka$. The mean iridium accumulation rate determined for the "gray clay" and the first 25 cm following the "gray clay" amounts to 1.22 ng $Ir/cm^2/Ka$ and decreases to 0.3 ng $Ir/cm^2/Ka$ in the overlying 100 cm of lower Danian chalks.

An obvious way to better understand the iridium chemistry in ancient sediments is by comparison with recent processes. Unfortunately, there is still comparatively meager data available from Holocene and Pleistocene sediments and even less is known of the biogeochemical pathways of iridium and other noble elements. The iridium accumulation rates reported for Holocene and Quaternary deep-sea sediments show a considerable range and seem strongly dependent on lithology and depositional environment. Kyte and Wasson (1986) reviewed the available data from red clays and considered an average accumulation rate of 0.014 ng $Ir/cm^2/Ka$ as typical. For carbonate environments, however, much higher iridium accumulation rates seem to prevail. For the Caribbean Core P 6304, an iridium accumulation rate of 0.8 ng $Ir/cm^2/Ka$ was calculated (Crocket and Kuo, 1979). An iridium accumulation rate of 4.4 ng $Ir/cm^2/Ka$ can be determined for the carbonate oozes at Manop Site C in the eastern equatorial Pacific (Goldberg et al., 1986; Prahl et al., 1989). The highest iridium accumulation rate currently known to us is >10 ng $Ir/cm^2/Ka$ in hemipelagic Holocene sediments of the Santa Barbara Basin, which contain a mere 0.2 ppb Ir (Goldberg et al., 1986) but accumulate rather rapidly (Bruland et al., 1974). These latter values are within or above the range of iridium accumulation rates calculated for the Cretaceous/Tertiary boundary interval at Site 738. The increase in the iridium (and other element) concentrations by a factor of 60 or so could thus be caused in large part by the decrease in the supply of detrital and carbonate dilutants.

There remain numerous difficulties in interpretations of high-resolution stratigraphic results of the geochemistry. The few indications for possibly higher iridium accumulation in recent marine sediments than hitherto assumed is certainly one of them. Other difficulties arise from the fact that the trace element concentrations are extremely low and the danger of contamination accordingly high. In addition, various laboratories employ different analytical techniques, which may lead to divergent results and thus generally require duplicate measurements by a second laboratory before they can be accepted. Unfortunately, the measurements indicating high iridium accumulation in Holocene sediments have not been confirmed independently yet.

If these high Holocene and Quaternary iridium accumulation rates are considered characteristic for carbonate and/or coastal depositional environments, then the time required to deposit the total of 320 ng Ir/cm^2 encountered in the carbonate-rich, shallow-water Cretaceous/Tertiary boundary interval at Site 738 would be 32,000 yr (assuming an accumulation rate of 10 ng $Ir/cm^2/Ka$ as in the Santa Barbara Basin), or 73,000 yr (assuming an accumulation rate of 4.4 ng $Ir/cm^2/Ka$ as in the eastern equatorial Pacific), or 400,000 yr (assuming an accumulation rate of 0.8 ng $Ir/cm^2/Ka$ as in the Caribbean Sea). Should these higher Holocene background accumulation rates of iridium in carbonate environments be confirmed in the future, then there would be little left of the excess accumulation of noble elements and metals in many other marine Cretaceous/Tertiary boundary sections (Thierstein, 1982: table 5), which have considerably lower iridium concentrations than Site 738. Consequently, there would be no need to appeal to extraterrestrial or extraordinary volcanic events to account for the total mass accumulation of iridium (and other metals).

In addition, the dramatic decrease of the bulk sediment accumulation rate in the laminated interval at Site 738 by a factor of 17 would lead by itself to a proportional increase in the concentrations of iridium and other elements if their fluxes had remained constant. Similar drops in the sedimentation rates in other sections have also been suggested.

Even allowing for significant changes in the dilution factor across the Cretaceous/Tertiary boundary, there still seems to be an excess iridium over background at Site 738 and in many other sections which still would require an explanation. How could the rates of iridium deposition be shifted so dramatically? Could there be transitional reservoirs for iridium and other metals in the exogenic cycle?

Iridium in the Hydrosphere

Knowing that the global marine biosphere was seriously disturbed at the time, as evidenced by (1) well-documented taxonomic changes in marine microfossils, (2) the drop in biogenic carbonate supply, and (3) the carbon isotopic shift, could an enhancement of microbial activity and/or changes in the overall

[8] Note added in proof: Recent new results from Samples 119-738C-22R-1, 10–11 cm, 119-738C-22R-1, 115–116 cm, and 119-738C-22R-3, 15–16 cm, have an average Ir content of 5.4 ± 1.7 ppt, which can be considered characteristic of Late Cretaceous background concentrations at this site (F. Asaro, pers. comm., 18 Sept. 1990).

ocean chemistry and associated element fluxes reasonably explain the observed iridium and other element concentration anomalies? This question has to be denied for two reasons. First, the excess noble element concentrations at the Cretaceous/Tertiary boundary are likely of mantle or extraterrestrial origin because their osmium isotopic compositions are closer to chondrites and ultramafics than to manganese nodules (Luck and Turekian, 1983). Second, new studies of the marine chemistry of iridium make such a source also unlikely, as the following arguments show.

The amount of iridium dissolved in seawater has recently been estimated as 2×10^{-15} g Ir per g seawater and the residence time of iridium in the oceans as about 1 m.y. (Goldberg et al., 1986). If there were worldwide environmental effects that would deposit iridium out of the present-day ocean at a rapid rate, the total iridium in a 5000-m-deep ocean with 2×10^{-15} g Ir per g seawater would be 10^{-9} g Ir/cm^2. This is 1/320th of the amount found at the Cretaceous/Tertiary boundary of Site 738 or 1/15th of the amount at Gubbio (Alvarez et al., 1980). With Goldberg et al.'s (1986) value for the residence time of iridium, it would take 13 m.y. at Site 738 and 0.6 m.y. at Gubbio to deposit that much iridium from the oceans by normal means. The excess iridium at the Cretaceous/Tertiary boundary could not, therefore, have been derived from the oceanic reservoir.

Iridium in the Biosphere

Recent studies of the iridium concentrations in marine and terrestrial plants provide some boundary conditions to evaluate the possibility that the destruction of a major part of the global biosphere may have released significant amounts of noble elements into the sediment reservoir. Today's living biosphere consists of approximately 3×10^{15} g C in the living marine biota and about 500×10^{15} g C in the living terrestrial biota (Bolin, 1986). Today a mass mortality of 90% of the global biosphere would thus lead to the release of about 450×10^{15} g C into the exogenic cycle. The mean iridium content of various marine organisms has been determined to range from <4 to 80×10^{-12} g Ir per g living matter with a mean of 20×10^{-12} g Ir per g living matter (Wells et al., 1988). The iridium content of potentially more important terrestrial plant matter is less well known. Wells et al. (1988) found 40×10^{-12} Ir per g living matter in an NBS standard consisting of dried orchard leaves, but they cite another determination by Valentine et al. (1982), who found much higher concentrations of 17 to 26×10^{-9} g Ir per g living matter in plants growing in mafic soils. Thus a mass mortality involving the short-term destruction of 90% of today's global biosphere would lead to the release of about 9×10^{7} g Ir (using the low estimate of 20 ppt Ir of Wells et al., 1988) and 9×10^{10} g Ir (using the high estimate of 20 ppb Ir of Valentine et al., 1982). The latter would be close to global excess iridium accumulation at the Cretaceous/Tertiary of approximately 3×10^{11} g Ir, which can be determined from the average excess iridium deposition of about 60 ng/cm^2 in over 25 marine and continental sections all over the world (Alvarez et al., 1982). If temporary recycling of iridium in the exogenic cycle is necessary to account for the drawn-out distribution of iridium in the non-bioturbated sedimentary section at Site 738, then the global biosphere, possibly including the organic carbon stored in soils, might be a conceivable reservoir. This reservoir, however, would have to store osmium with an isotopic composition similar to ultramafic or extraterrestrial rocks rather than manganese nodules. Clearly, additional studies of the noble element geochemistry of terrestrial plant and soil materials would be beneficial.

These arguments cannot be construed as evidence against an extraterrestrial impact at the Cretaceous/Tertiary boundary, because the latter receives independent support by the presence of altered tectites and shocked quartz grains in marine and continental sections (e.g., Bohor, 1990). The abundance and thus significance of such impact-related grains, however, remain controversial (Schmitz, 1990) and flux rate determinations (background and increases at the Cretaceous/Tertiary boundary) would clearly be instructive.

CALCAREOUS NANNOFOSSILS

The Cretaceous/Tertiary boundary is the most spectacular evolutionary event known within the well-documented 200-m.y. history of the calcareous phytoplankton. Because of their smallness and abundance, studies of the evolutionary population dynamics can be carried out at a very high stratigraphic resolution of millimeters to centimeters. A common limitation for evolutionary studies using nannofossils at the Cretaceous/Tertiary boundary in the past has often been the effect of bioturbation (e.g., Thierstein and Okada, 1979), which tends to smear out and attenuate changes in the original supply of sediment particles from the photic zone. Because the paleontologically defined Cretaceous/Tertiary boundary recovered at Site 738 occurs in a finely laminated interval, a detailed study of the calcareous nannofossil populations promised to provide a record of maximum stratigraphic resolution.

Light-Microscopic Analyses

The taxonomic compositions of the calcareous nannofossil assemblages are given in table 5 of Wei and Thierstein (this volume). For the Cretaceous/Tertiary boundary interval (i.e., Section 119-738C-20R-5, 50–103 cm), the relative abundances of individual taxa were determined quantitatively. Smear slides of samples taken with toothpicks during the initial description of the cores on board were studied under the light microscope. In all samples the proportion of intact nannofossils is less than 1% of all particles present (estimated in the light microscope). The majority (70%–99%) of the particles present consists of microcarbonate of a few microns in diameter (Fig. 1), and the remainder (1%–30%) consists of nannofossil fragments and clay particles. The nannofossils in these samples are moderately to strongly etched and slightly to moderately overgrown. Because of the scarcity of intact nannofossils and the mediocre preservation, only 100 specimens per sample were counted. As a result of the relatively small sample sizes, large statistical uncertainties exist with respect to the significance of the determined minor fluctuations among the individual taxa. Therefore, only the changes in the proportion of all latest Cretaceous vs. all earliest Tertiary nannofossil taxa were plotted in Figure 1. The taxa occurring consistently in the upper Maestrichtian chalks of Cores 119-738C-21R through -24R are considered to belong to the Cretaceous assemblages, and those taxa that have their first appearance in the boundary interval and persist into the earliest Danian assemblages of Cores 119-738C-19R and -18R are taken as belonging to the Tertiary assemblage (Table 2). All of the Maestrichtian and Danian nannofossils encountered at Site 738 have been reported previously from uppermost Cretaceous and lowermost Tertiary sediments elsewhere.

Among the first 100 intact nannofossil specimens examined in the smear slide of the "gray clay" at 96.1 cm, one fragment of *Thoracosphaera* sp. and one specimen of *Markalius inversus* (oval morphotype) were encountered. *Thoracosphaera* sp. is known to become dominant in the lowermost Danian assemblages at many low-latitude sections, although it is present in low abundances in the Upper Cretaceous (Thierstein, 1981). Some of the fragments identified in the light microscope as *Thoracosphaera* sp. may in fact belong to related calcareous dinoflagellate cysts (Pl. 6). *M. inversus*, generally dominated by circular rather than oval morphotypes, is also considered a Danian species, although one specimen was recorded in Section 119-738C-23-1, 84 cm (late Maestrichtian), and very rare exam-

Table 2. Nannofossil taxa considered to belong to Late Cretaceous and early Tertiary assemblages.

Late Cretaceous	early Tertiary
Ahmuellerella octoradiata	*Biantholithus sparsus*
Arkhangelskiella cymbiformis	*Cruciplacolithus primus*
Biscutum constans	*Cruciplacolithus tenuis*
Biscutum magnum	*Hornibrookina teuriensis*
Chiastozygus litterarius	*Markalius inversus* (circular morphotype)
Cretarhabdus conicus	*Markalius inversus* (oval morphotype)
Cretarhabdus surirellus	*Prinsius dimorphosus*
Cribrosphaerella daniae	*Thoracosphaera* sp.
Cribrosphaerella ehrenbergii	*Toweius* sp.
Cyclagelosphaera reinhardtii	*Zygodiscus sigmoides*
Eiffellithus turriseiffeli	
Gartnerago obliquum	
Kamptnerius magnificus	
Lithraphidites carniolensis	
Lucianorhabdus cayeuxii	
Micula staurophora	
Nephrolithus frequens	
Prediscosphaera cretacea	
Prediscosphaera stoveri	
Reinhardtites anthophorus	
Watznaueria barnesae	
Zygodiscus spiralis	

ples were also observed sporadically in upper Maestrichtian assemblages elsewhere (Thierstein, 1981). Further examination of the assemblages in the "gray clay" and in the whitish ooze layer at 95.9 cm immediately above the "gray clay" has revealed additional fragments of *Thoracosphaera* sp., with one specimen of *M. inversus* in the scanning electron microscope (SEM) (Pl. 5, Fig. 3) and one specimen each of *Toweius* sp. and *Cruciplacolithus tenuis*. The latter two taxa are known to have their first appearance above the Cretaceous/Tertiary boundary within the upper part of Magnetosubchron 29R and the lower part of the foraminifer *S. pseudobulloides* Zone in the Bottaccione section at Gubbio (Roggenthen and Napoleone, 1977; Monechi and Thierstein, 1985) and in other Cretaceous/Tertiary boundary sections, such as at El Kef (Perch-Nielsen, 1981). The first continued occurrences of *Toweius* sp. and *C. tenuis* at this site are at Samples 119-738C-20R-5, 60 cm, and 119-738C-20R-5, 70.5 cm, respectively (i.e., 14–24 cm above the "gray clay"). The isolated specimens of *M. inversus* and *Toweius* sp. may therefore be contaminants from higher up in the core. In fact, white and soft sediment is observable along the margins of the recovered split core (barely visible in Figure 1 but confirmed by additional toothpick sampling and onboard examination of, for instance, the white, millimeter-sized sediment piece discernible on the left side of the core half at 95.1–95.6 cm). Such displaced sediment may also have been squeezed into cracks that developed during the drilling operations. No Danian specimens were encountered in any of the three samples between 95.7 and 94.2 cm. From Sample 119-738C-20R-5, 92 cm, upward the Danian species occur continuously and their proportion increases from a few percent to 85% at 80.2 cm, with a renewed increase of the (reworked) Cretaceous taxa above that level.

SEM Analyses of the "Gray Clay"

The SEM examination of the surface of a freshly broken chip of the "gray clay" (Sample 119-738C-20R-5, 96.0–96.2 cm) revealed, compared with other samples above and below, an increased abundance of foraminiferal and calcispherulid tests, which are usually filled with relatively well-preserved and intact nannofossils (Pls. 1–3). Nannofossils occur in the surrounding clayey matrix as well, but they are generally more fragmented and less well preserved. All nannofossil specimens identified in the SEM in the "gray clay" sample belong to the latest Maestrichtian assemblages.

SEM Analyses of Individual Laminae

For a better understanding of the character of the laminae, a few undisturbed, intact sediment pieces from above and below the "gray clay" (i.e., Samples 119-738C-20R-5, 84–85 cm; 119-738C-20R-5, 89–90 cm; 119-738C-20R-5, 93–94 cm; 119-738C-20R-5, 94–95 cm; 119-738C-20R-5, 95–96 cm; and 119-738C-20R-5, 97–98 cm) were broken and the surfaces examined under the SEM. The differences between the light green and the white laminae are subtle and appear to consist of an observable change in the ratio of recognizable nannofossils and nannofossil fragments vs. an apparently coherent matrix of seemingly cohesive clay minerals (Pls. 4 and 5). Although shelled foraminifers and their casts were observed in some samples, their frequency was much lower ($<10\times$) than in the "gray clay" layer.

FORAMINIFERS

Recovery of undisturbed, finely laminated sediments immediately above and below the "gray clay" in Hole 738C provides a unique opportunity to elucidate the pattern of planktonic and benthic foraminifer extinction and survivorship during the terminal Cretaceous biotic crisis event. Other deep-sea sections that yield a stratigraphically complete record of deposition across this boundary show evidence of intense bioturbation (e.g., Stott and Kennett, 1990), sediment reworking (Smith and Poore, 1984), or downslope slumping (Gerstel et al., 1986). Presence of the laminated Cretaceous/Tertiary sequence at Hole 738C eliminates bioturbation as a factor influencing the foraminifer distributions and diminishes the likelihood of reworking due to bottom current scour. Sieved residues of the >45-μm fraction were analyzed from samples taken at 1-cm intervals between 82 and 102 cm in Section 119-738C-20R-5 and at 10-cm intervals to the top of that section. Distribution data for benthic and planktonic foraminifers and other biogenic and nonbiogenic constituents observed throughout this sequence are presented by Huber in his table 2 (this volume). Lists of upper Maestrichtian, lower Danian, and "survivor" species occurring in Cores 119-738C-18R through -21R are shown in Tables 3 and 4.

Samples from below the "gray clay" (i.e., Sample 119-738C-20R-5, 96.3–102 cm) were especially resistant to disaggregation techniques because of a strong degree of sediment lithification. Thus, only presence/absence information was obtained for this interval. Foraminifers are especially rare in the interval from Section 119-738C-20R-5, 96.3–100 cm. Quantitative estimates

Table 3. Late Maestrichtian and early Danian benthic foraminifer species occurring at Hole 738C.

Preboundary species (Core 119-738C-21R and below)	Cretaceous-Tertiary species (Laminated interval of Section 119-738C-21R-5, 83–98 cm)
Bolivinoides draco	*Alabamina creta*
Frondicularia sp. 1	*Bolivinoides laevigata*
Frondicularia sp. 2	*Buliminella* sp.
Gavelinella eriksdalensis	*Cibicides* sp.
Neoflabellina praereticulata	*Conorbina* sp.
Nodosaria multicostata	*Coryphostoma incrassata*
	Dentalina sp.
	Epistominella sp.
	Gavelinella beccariformis[a]
	Gavelinella sp.
	Lenticulina sp.
	Nuttallides truempyi[a]
	Praebulimina reussi
	Pullenia coryelli
	Spiroplectammina sp.
	Stilostomella subspinosa

[a] Denotes common occurrence.

Table 4. Late Maestrichtian, Danian, and reworked planktonic foraminifer species occurring at Hole 738C.

Late Maestrichtian species becoming extinct	Reworked Maestrichtian species	Danian descendant species
Abathomphalus mayaroensis	*Globigerinelloides multispinatus*	*Bifarina alabamensis*
Archaeoglobigerina australis	*Globigerinelloides subcarinata*	*Chiloguembelina crinita*
Globotruncanella havanensis	*Gublerina robusta*	*Chiloguembelina waiparensis*
Hedbergella sliteri	*Guembelitria cretacea*	*Eoglobigerina fringa*
Heterohelix planata	*Heterohelix dentata*	*Eoglobigerina triloba*
	Heterohelix globulosa	*Eoglobigerina*? cf. *caravacaensis*
		Eoglobigerina? sp.
		Subbotina minutula
		Zeauviperina teuria

of relative abundance were determined for samples from above the "gray clay" (i.e., Section 119-738C-20R-5, 4–96 cm) based on 100 specimen counts per sample. Rare occurrence and inadequate preservation of foraminifers preclude a more statistically accurate characterization of the faunal changes that occur in the lower Danian sediments.

Careful analysis of the sieved residues revealed no grains of shocked quartz or the presence of volcaniclastic and terrigenous clastic grains. Pyrite framboids were observed 2–4 cm above the Cretaceous/Tertiary boundary clay, but these are very small in size and occur in very low numbers. Glauconite was not observed within this sequence. The dominant biogenic constituents from the Cretaceous/Tertiary laminated interval predominantly include pithonellid calcispheres, whereas planktonic and benthic foraminifers were rare in comparison.

Benthic Foraminifers

A significant change in upper Maestrichtian benthic foraminifer assemblages occurs below the "gray clay," between Samples 119-738C-20R-CC and 119-738C-21R-1 (377.4–379.9 mbsf). *Bolivinoides draco, Neoflabellina praereticulata, Frondicularia* spp., and several nodosariids all have their last occurrence within or just below this unrecovered interval. The sieved residues and sediment aggregates from samples from the interval in Section 119-738C-20R-5, 96–102 cm, reveal that overall benthic foraminifer test size and species diversity are diminished compared to the older Maestrichtian benthic assemblages. The dominant benthic foraminifer species observed from Samples 119-738C-20R-CC through 119-738C-20R-5, 4–5 cm, include *Gavelinella beccariiformis, Nuttallides truempyi, Bolivinoides laevigata*, and *Alabamina creta*. Although benthic assemblages from immediately below and above the "gray clay" show no significant difference in taxonomic composition, poor preservation within this interval precludes a concise documentation of the taxonomic and morphologic changes that may have occurred.

Planktonic Foraminifers

Although the upper Maestrichtian planktonic foraminifer *Abathomphalus mayaroensis* occurs consistently in samples from Cores 119-738C-23R to -21R, this species was not found in Maestrichtian samples from Core 119-738C-20R. These samples primarily yield diminutive specimens of the Upper Cretaceous species *Heterohelix globulosus, Globigerinelloides multispinatus*, and *Globigerinelloides subcarinatus.* Rare specimens of *Globotruncanella petaloidea* and *Gublerina robusta* were found in Sample 119-738C-20R-CC, but not in the overlying Maestrichtian samples.

Several biserial planktonic foraminifer specimens occurring in Sample 119-738C-20R-5, 100–101 cm, show distinctive morphologic characteristics that warrant their classification in the Tertiary genus *Chiloguembelina.* Asymmetry of the aperture and absence of longitudinal costellae clearly distinguish these forms from the Cretaceous biserial genus *Heterohelix.* Although the small size ($< 100\ \mu m$) and rare abundance of these forms would suggest the possibility of downhole contamination, the near-central position of the asymmetric aperture indicates that these represent an evolutionary link between Maestrichtian and Danian heterohelicids (see Huber, this volume).

The early Danian P1a Zone is recognized from the Cretaceous/Tertiary boundary clay to Sample 119-738C-20R-4, 130–131 cm, based on the occurrence of *Eoglobigerina fringa, Eoglobigerina minutula*, and *Eoglobigerina*? cf. *caravacaensis* and absence of *Subbotina pseudobulloides* and *Globoconusa daubjergensis.* The latter two species first occur in Sample 119-738C-20R-4, 130–131 cm, and range up through Core 119-738C-17R. Absence of the nominal taxon of the P1a Zone, *Parvulorugoglobigerina eugubina*, may be the result of paleobiogeographic exclusion of this species from the Antarctic region (Stott and Kennett, 1990). *Zeauvigerina teuria, Bifarina alabamensis*, and *Eoglobigerina triloba* first appear within this zone in Section 119-738C-20R-5. Planktonic specimens occurring within the P1a Zone at Hole 738C are mostly smaller than 100 μm, are moderately to poorly preserved, and are dominated by *Chiloguembelina crinita.*

The stratigraphic ranges of six Maestrichtian planktonic foraminifer species extend to within the laminated sediments above the "gray clay" and/or in stratigraphically higher Danian samples. These species are listed in Table 4. Whether the occurrences of Cretaceous species within the laminated Danian sediments are due to current reworking or species survivorship cannot be determined until they are analyzed for their stable isotopic composition and compared with the stable isotopic values of co-occurring Danian species. Although close observation of the laminated sediments reveals no evidence for bottom current scouring, pelagic rain of older sediments reworked from the nearby source cannot be ruled out.

Discussion

The occurrence of Tertiary planktonic foraminifer morphotypes within uppermost Maestrichtian sediments at Hole 738C suggests that ecological stress was already prevalent within the surface and bottom waters prior to the iridium enrichment event. This conclusion is supported by several other criteria, including (1) disappearance of several distinctive benthic foraminifer species within 3 m below the Cretaceous/Tertiary boundary, (2) loss of keeled planktonic foraminifers within 0–2 m below the Cretaceous/Tertiary boundary, and (3) appearance of laminae and hence, loss of benthic bioturbation 2 cm below the "gray clay." It is not possible to know the time span represented by these changes because of the poor magnetostratigraphic control and poor core recovery below the Cretaceous/Tertiary boundary clay. Nor is it possible to quantify the faunal turnover that occurs within this interval because of the poor foraminifer preservation. Nevertheless, the patterns of extinction and inferred survivorship observed at Hole 738C are consistent with the results of Keller (1988a, 1988b, 1989), who recognized extended periods of planktonic and benthic foraminifer extinction and survivorship from about 300,000 yr below to 200,000–300,000 yr above Cretaceous/Tertiary boundaries at El Kef, Tunisia, and the Brazos River, Texas. Future studies of the stable isotopic composition of individual foraminifer taxa and thin-section study of the Hole 738C sequence may further elucidate the biotic and ecologic changes that occur in this Antarctic sequence.

STABLE ISOTOPES

In the absence of suitable numbers of isolated foraminifers, only the fine fractions (<38 μm) were analyzed for the oxygen and carbon isotopic ratios. The preparation procedure was that described by Thierstein and Woodward (1981) and the measurements were made with the VG 903 mass spectrometer in the stable isotope laboratory of the Geological Institute, ETH-Zürich. The results are given relative to the PDB standard and are listed in Table 1 and plotted in Figure 1.

The oxygen isotopic values across the Cretaceous/Tertiary boundary do not show large changes, although the average ratios in the nonbioturbated and more clayey interval are more negative by about 0.4‰ than the Upper Cretaceous and lower Paleocene chalks. The total carbon isotopic variability in this interval is around 1‰. The Upper Cretaceous chalks have values around 2.15‰ and then, after a slight decrease in the nonbioturbated chalk 2 cm below the "gray clay," the values increase to around 2.4‰ in the laminated interval immediately above the "gray clay." Subsequently, they show a decrease to 1.5‰ in the lowermost Danian chalks (Fig. 1).

An interpretation of the stable isotopic values of Hole 738C directly in paleoceanographic terms cannot be justified, as the dominant signal carrier is not biogenic but consists dominantly of microcarbonate of unknown origin. Studies of the <38-μm fractions in well-preserved, diagenetically altered sediment sequences have demonstrated the variability of stable isotopic ratios related to changes in taxonomic composition (Paull and Thierstein, 1987), dissolution (Paull et al., 1988), and diagenetic effects (Thierstein, 1983; Thierstein and Roth, in press). Nevertheless, the somewhat less positive values measured in the chalks above the laminated interval (377.0–376.0 mbsf) correlate well with the negative $\delta^{13}C$ excursions observed in other Cretaceous/Tertiary boundary sections in the Tertiary part of Chron 29R and the lower part of Chron 29N (e.g., Thierstein and Berger, 1978; Stott and Kennett, 1989). We take this as additional evidence that the time interval immediately following the Cretaceous/Tertiary boundary is indeed represented by sediments at Hole 738C.

CONCLUSIONS

An interpretation of the events and processes leading to the Cretaceous/Tertiary boundary record at Hole 738C does not seem any less enigmatic than in other sections. The more salient features of this section are the following:

1. Despite the fact that the iridium event and the evolutionary change in the nannofossil assemblage occur in a nonbioturbated or laminated interval, both tracers record the presumably sudden and "catastrophic" Cretaceous/Tertiary boundary event over an interval of at least several centimeters of sediment thickness.

2. Interestingly, bioturbation of the late Maestrichtian chalks ceases a few centimeters below the level of a distinct, 2-mm-thick "gray clay" layer considered to mark the Cretaceous/Tertiary boundary.

3. The "gray clay" layer shows the highest iridium value (18 ppb of bulk sediment) measured in this section; however, the iridium contents of the uppermost Maestrichtian chalks are strongly enriched (1.65 ppb) relative to the iridium contents of the Danian chalks (0.1–0.3 ppb) 1 m higher. (See note added in proof.)

4. No faunal, mineralogical, or chemical evidence for anoxia was found.

5. Despite the dominance of microcarbonate particles of diagenetic or detrital origin, the earliest Tertiary taxa are recorded immediately above the "gray clay" layer and rise gradually to 85% of the recognized nannofossil specimens over an interval of 16 cm of finely laminated clays that overlie the "gray clay."

6. There is no significant, recognizable change in the composition of the smectite-dominated clay mineral assemblage in the transition.

7. Although the clays and many metals show concentration increases at the Cretaceous/Tertiary boundary, the available chronology and bulk accumulation rates suggest that the observed anomalies may not be caused entirely by an increased influx of metals, but could be the result of a significant decrease in the supply of detrital and biogenous particles.

8. Most other paleontological and geochemical tracers show features and signals similar to those observed in other marine sections.

ACKNOWLEDGMENTS

We thank Cinzia Cervato (ETH) for analyses of the stable isotopes and Urs Gerber (ETH) for photographic work. Discussion and critical remarks on manuscript drafts by Heinz Hilbrecht (ETH) are acknowledged. Financial support was provided by grant Fu 119/15 (to WUE) of the Deutsche Forschungsgemeinschaft and by the Swiss National Science Foundation to HRT. Financial support for FA and HVM was provided predominantly by the Office of Basic Energy Sciences of the U.S. Department of Energy under Contract No. DE-AC03-76SF00098 and also by the U.S. National Aeronautics and Space under Contract No. A-59508C. Construction of the Iridium Coincidence Spectrometer was made possible primarily by grants from the M. J. Murdock Charitable Trust in Vancouver, Washington.

This is Alfred Wegener Institute Contribution No. 275.

REFERENCES

Alvarez, L. W., Alvarez, W., Asaro, F., and Michel, H. V., 1980. Extraterrestrial cause for the Cretaceous-Tertiary extinction. *Science*, 208: 1095–1108.

________, 1982. Current status of the impact theory for the terminal Cretaceous extinction. *In* Silver, L. T., and Schultz, P. H. (Eds.), *Geological Implications of Impacts of Large Asteroids and Comets on the Earth.* Spec. Pap. Geol. Soc. Am., 190:305–315.

Barker, P. F., Kennett, J. P., et al., 1988. *Proc. ODP, Init. Repts.*, 113: College Station, TX (Ocean Drilling Program).

Barron, J., Larsen, B., et al., 1989. *Proc. ODP, Init. Repts.*, 119: College Station, TX (Ocean Drilling Program).

Berggren, W. A., Kent, D. V., and Flynn, J. J., 1985. Jurassic to Paleogene: Part 2. Paleogene geochronology and chronostratigraphy. *In* Snelling, N. J. (Ed.), *The Chronology of the Geological Record.* Geol. Soc. London Mem., 10:141–195.

Biscaye, P. E., 1964. Distinction between kaolinite and chlorite in recent sediments by X-ray diffraction. *Am. Miner.*, 49:1281–1289.

________, 1965. Mineralogy and sedimentation of recent deep-sea clays in the Atlantic Ocean and adjacent seas and oceans. *Geol. Soc. Am. Bull.*, 76:803–832.

Bohor, B. F., 1990. Comment and reply on "Origin of microlayering in worldwide distributed Ir-rich marine Cretaceous/Tertiary boundary clays." *Geology*, 18:88–89.

Bolin, B., 1986. How much CO_2 will remain in the atmosphere? *In* Bolin, B., Döös, B. R., Jäger, J., and Warrick, R. A. (Eds.), *The Greenhouse Effect, Climatic Change, and Ecosystems.* SCOPE 29: Chichester (Wiley), 93–155.

Bruland, K. W., Bertine, K., Koide, M., and Goldberg, E. D., 1974. History of metal pollution in Southern California coastal zone. *Environ. Sci. Technol.*, 8:425–432.

Chave, A., 1984. Lower Paleocene-Upper Cretaceous magnetostratigraphy, Site 525, 527, 528, and 529, Deep Sea Drilling Project Leg 74. *In* Moore, T. C. Jr., Rabinowitz, P. D., et al., *Init. Repts. DSDP*, 74: Washington (U.S. Govt. Printing Office), 525–531.

Crocket, J. H., and Kuo, H. Y., 1979. Sources for gold, palladium and iridium in deep-sea sediments. *Geochim. Cosmochim. Acta*, 43: 831–842.

Dyer, B. D., Lyalikova, N. N., Murray, D., Doyle, M., Kolesov, G. M., and Krumbein, W. E., 1989. Role of microorganisms in the formation of iridium anomalies. *Geology*, 17:1036–1039.

Elliott, W. C., Aronson, J. L., Millard, H. T. and Gierlowski-Kordesch, E., 1989. The origin of the clay minerals at the Cretaceous/Tertiary boundary in Denmark. *Geol. Soc. Am. Bull.*, 101:702–710.

Fütterer, D. K., 1990. Distribution of calcareous dinoflagellates at the Cretaceous-Tertiary boundary of Queen Maud Rise, eastern Weddell Sea Antarctica (ODP Leg 113). *In* Barker, P. F., Kennett, J. P., et al., *Proc. ODP, Sci. Results*, 113: Washington (U.S. Govt. Printing Office), 533–538.

Gerstel, J., Thunell, R. C., Zachos, J. C., and Arthur, M. A., 1986. The Cretaceous/Tertiary boundary event in the North Pacific: planktonic foraminiferal results from Deep Sea Drilling Project Site 577, Shatsky Rise. *Paleoceanography*, 1:97–117.

Goldberg, E. D., Hodge, V., Kay, P., Stallard, M., and Koide, M., 1986. Some comparative marine chemistries of platinum and iridium. *Appl. Geochem.*, 1:227–232.

Hamilton, N., and Susyumov, A. E., 1983. Late Cretaceous magnetostratigraphy of Site 516, Rio Grande Rise, southwestern Atlantic Ocean, Deep Sea Drilling Project, Leg 72. *In* Barker, P. F., Carlson, R. L., Johnson, D. A., et al., *Init. Repts. DSDP*, 72: Washington (U.S. Govt. Printing Office), 723–730.

Herbert, T. D., and D'Hondt, S., 1990. Precessional climate cyclicity in Late Cretaceous–early Tertiary marine sediments: a high-resolution chronometer of Cretaceous–Tertiary boundary events. *Earth Planet. Sci. Lett.*, 99:263–275.

Izett, G. A., and Bohor, B. F., 1987. Comment and reply on "Dynamic deformation of volcanic ejecta from the Toba caldera: possible relevance to Cretaceous/Tertiary boundary phenomena." *Geology*, 15: 90.

Johnsson, M. J., and Reynolds, R. C., 1986. Clay mineralogy of shale-limestone rhythmites in the Scaglia Rossa (Turonian-Eocene), Italian Apennines. *J. Sediment. Petrol.*, 56:501–509.

Kastner, M., Asaro, F., Michel, H. V., Alvarez, W., and Alvarez, L. W., 1984. The precursor of the Cretaceous-Tertiary boundary clays at Stevns Klint, Denmark, and DSDP Hole 465A. *Science*, 226:137–143.

Keller, G., 1988a. Biotic turnover in benthic foraminifera across the Cretaceous/Tertiary boundary at El Kef, Tunisia. *Palaeogeogr., Palaeoclimatol., Palaeoecol.*, 66:153–171.

________, 1988b. Extinction, survivorship and evolution of planktic foraminifera across the Cretaceous/Tertiary boundary at El Kef, Tunisia. *Mar. Micropaleontol.*, 13:239–263.

________, 1989. Extended period of extinctions across the Cretaceous/Tertiary boundary in planktonic foraminifera of continental shelf sections: implications for impact and volcanism theories. *Geol. Soc. Am. Bull.*, 101:1408–1419.

Kyte, F. T., and Wasson, J. T., 1986. Accretion rate of extraterrestrial matter: iridium deposited 33 to 67 million years ago. *Science*, 232: 1225–1229.

Lange, H., 1982. Distribution of chlorite and kaolinite in eastern Atlantic sediments off North Africa. *Sedimentology*, 29:427–432.

Lowrie, W. R., Alvarez, W., Napoleone, G., Perch-Nielsen, K., Premoli Silva, I., and Toumarkine, M., 1982. Paleogene magnetic stratigraphy in Umbrain pelagic carbonate rocks: the Contessa sections, Gubbio. *Geol. Soc. Am. Bull.*, 93:414–432.

Luck, J. M., and Turekian, K. K., 1983. Osmium-187/Osmium-186 in manganese nodules and the Cretaceous-Tertiary boundary. *Science*, 22:613–615.

Manivit, H., 1984. Paleogene and Upper Cretaceous calcareous nannofossils from Deep Sea Drilling Project Leg 74. *In* Moore, T. C., Jr., Rabinowitz, P. D., et al., *Init. Repts. DSDP*, 74: Washington (U.S. Govt. Printing Office), 475–499.

Manivit, H., and Feinberg, H., 1984. Correlation of magnetostratigraphy and nannofossil biostratigraphy in Upper Cretaceous and Lower Paleocene sediments of the Walvis Ridge area. *In* Moore, T. C., Jr., Rabinowitz, P. D., et al., *Init. Repts. DSDP*, 74: Washington (U.S. Govt. Printing Office), 469–474.

Monechi, S., and Thierstein, H. R., 1985. Late Cretaceous-Eocene nannofossil and magnetostratigraphic correlations near Gubbio, Italy. *Mar. Micropaleontol.*, 9:419–440.

Monechi, S., Bleil, U., and Backman, J., 1985. Magnetobiochronology of Late Cretaceous-Paleogene and Late Cenozoic pelagic sedimentary sequences from the Northwest Pacific (Deep Sea Drilling Project, Leg 86, Site 577). *In* Heath, G. R., Burckle, L. H., et al., *Init. Repts. DSDP*, 86: Washington (U.S. Govt. Printing Office), 787–797.

Paull, C. K., and Thierstein, H. R., 1987. Stable isotopic fractionation among coccolith-sized particles in Quaternary deep-sea sediments. *Paleoceanography*, 2:423-429.

Paull, C. K., Hills, S. J., and Thierstein, H. R., 1988. Progressive dissolution of fine carbonate particles in pelagic sediments. *Mar. Geol.*, 81:27–40.

Peirce, J., Weissel, J., et al., 1989. *Proc. ODP, Init. Repts.*, 121: College Station, TX (Ocean Drilling Program).

Perch-Nielsen, K., 1981. Nouvelles observations sur les nannofossiles calcaires à la limite Crétacé-Tertiaire près de El Kef (Tunisie). *Cah. Micropaleont.*, 3:25–36.

Prahl, F. G., Muehlhausen, L. A., and Lyle, M., 1989. An organic geochemical assessment of oceanographic conditions at MANOP Site C over the past 26,000 years. *Paleoceanography*, 4:495–510.

Pujol, C., 1983. Cenozoic planktonic foraminiferal biostratigraphy of the southwestern Atlantic (Rio Grande rise): Deep Sea Drilling Project Leg 72. *In* Barker, P. F., Carlson, R. L., Johnson, D. A., et al., *Init. Repts. DSDP*, 72: Washington (U.S. Govt. Printing Office), 623–673.

Rampino, M. R., and Reynolds, R. C., 1983. Clay mineralogy of the Cretaceous-Tertiary boundary clay. *Science*, 219:495–498.

Reynolds, R. C., 1980. Interstratified clay minerals. *In* Brindley, G. W., and Brown, G. (Eds.), *Crystal Structures of Clay Minerals and their X-Ray Identification*. Mineral. Soc. Monogr. No. 5 (London):249–303.

Reynolds, R. C., and Hower, J., 1970. The nature of interlayering in mixed-layer illite-montmorillonites. *Clays Clay Miner.*, 18:25–36.

Roggenthen, W. M., and Napoleone, G., 1977. Upper Cretaceous-Paleocene magnetic stratigraphy at Gubbio, Italy. IV. Upper Maestrichtian-Paleocene magnetic stratigraphy. *Geol. Soc. Am. Bull.*, 88: 378–382.

Schmitz, B., 1988. Origin of microlayering in worldwide distributed Ir-rich marine Cretaceous/Tertiary boundary clays. *Geology*, 16:1068–1072.

________, 1990. Comment and reply on "Origin of microlayering in worldwide distributed Ir-rich marine Cretaceous/Tertiary boundary clays". *Geology*, 18:89–92.

Schmitz, B., Andersson, P., and Dahl, J., 1988. Iridium, sulfur isotopes and rare earth elements in the Cretaceous-Tertiary boundary clay at Stevns Klint, Denmark. *Geochim. Cosmochim. Acta*, 49:229–236.

Shipboard Scientific Party, 1989. Site 738. *In* Barron, J., Larsen, B., et al., *Proc. ODP, Init. Repts.*, 119: College Station, TX (Ocean Drilling Program), 229–288.

Smith, C. H., and Poore, R. G., 1984. Upper Maestrichtian and Paleocene planktonic foraminiferal biostratigraphy of the northern Cape Basin, Deep Sea Drilling Project Hole 524. *In* Hsü, K. J., LaBrecque, J. L., et al., *Init. Repts. DSDP*, 73: Washington (U.S. Govt. Printing Office), 449–457.

Stott, L. C., and Kennett, J. P., 1989. New constraints on early Tertiary palaeoproductivity from carbon isotopes in foraminifera. *Nature*, 342:526–529.

________, 1990. Antarctic Paleogene planktonic foraminifer biostratigraphy: ODP Leg 113, Sites 689 and 690. *In* Barker, P. F., Kennett, J. P., et al., *Proc. ODP, Sci. Results*, 113: Washington (U.S. Govt. Printing Office), 549–569.

Thierstein, H. R., 1981. Late Cretaceous nannoplankton and the change at the Cretaceous-Tertiary boundary. *In* Warme, J. E., et al. (Eds.), *The Deep Sea Drilling Project: A Decade of Progress*: Soc. Econ. Paleontol. Mineral., Spec. Publ., 32:355–394.

________, 1982. Terminal Cretaceous plankton extinctions: A critical assessment. *In* Silver, L. T., and Schultz, P. H., *Geological Implications of Impacts of Large Asteroids and Comets on the Earth*. Spec. Pap. Geol. Soc. Am., 190:385–405.

———, 1983. Oxygen and carbon isotopic fluctuations in cyclic mid-Cretaceous deep-sea sediments: Dominance of diagenetic effects. *Eos*, 64:733.

Thierstein, H. R., and Berger, W. H., 1978. Injection events in ocean history. *Nature*, 276:461–466.

Thierstein, H. R., and Okada, H., 1979. The Cretaceous/Tertiary boundary event in the North Atlantic. *In* Tucholke, B. E., Vogt, P. R., et al., *Init. Reports, DSDP*, 43: Washington (U.S. Govt. Printing Office), 601–616.

Thierstein, H. R., and Roth, P. H., in press. Stable isotopic and carbonate cyclicity in Lower Cretaceous deep-sea sediments: dominance of diagenetic effects. *Mar. Geol.*

Thierstein, H. R., and Woodward, D. L., 1981. Paleontological, stratigraphic, sedimentological, geochemical, and paleogeographical data of Upper Cretaceous and lowermost Tertiary sediment samples. *Scripps Inst. Oceanogr. Reference Ser.*, 81–82.

Valentine, I. M., Minski, M. J., and Peterson, P. J., 1982. Neutron activation analysis of noble metals in vegetation. *J. Radioanal. Chem.*, 71:115–127.

Wallace, M. W., Gostin, V. A., and Keays, R. R., 1990. Acraman impact ejecta and host shales: evidence for low-temperature mobilization of iridium and other platinoids. *Geology*, 18:132–135.

Wells, M. C., Boothe, P. N., and Presley, B. J., 1988. Iridium in marine organisms. *Geochim. Cosmochim. Acta*, 52:1737–1739.

Wise, S. W., Jr., and Wind, F. H., 1977. Mesozoic and Cenozoic calcareous nannofossils recovered by DSDP Leg 36 drilling on the Falkland Plateau, Southwest Atlantic sector of the Southern Ocean. *In* Barker, P., Dalziel, I.W.D., et al., *Init. Repts. DSDP*, 36: Washington (U.S. Govt. Printing Office), 269–492.

Date of initial receipt: 2 January 1990
Date of acceptance: 5 July 1990
Ms 119B-157

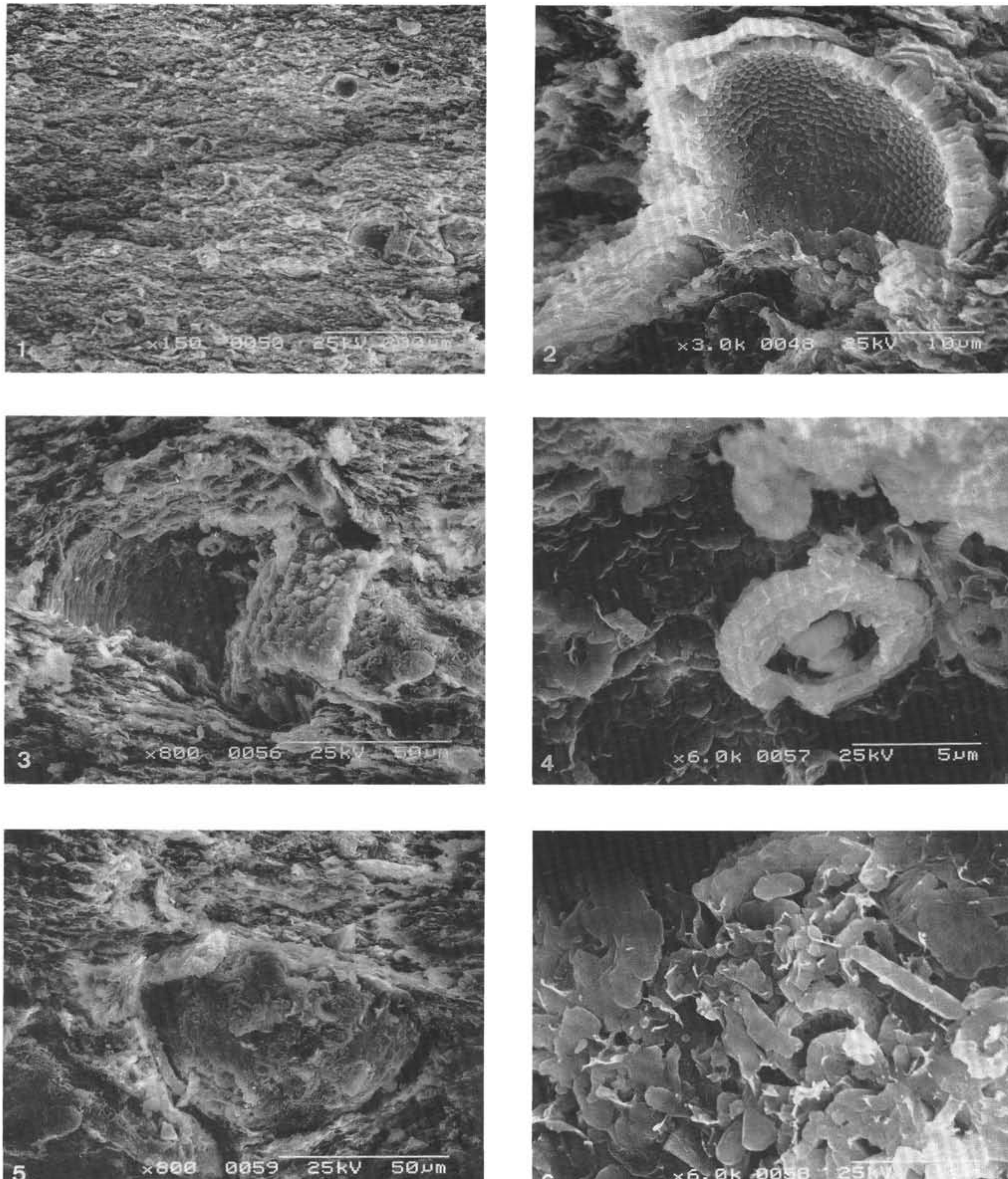

Plate 1. Cretaceous/Tertiary boundary clay (Sample 119-738C-20R-5, 96.0–96.2 cm). **1.** SEM photomicrographs of the Cretaceous/Tertiary boundary clay showing sedimentary microfabric with foraminifer and calcareous dinoflagellate remains. Three areas shown in Figure 1 are progressively enlarged in Figures 2–6. **2.** Well-preserved calcified dinoflagellate cyst, *Orthopithonella congruenta* Fütterer (1990). Embedded in the surrounding clay matrix are shields and fragments of Late Cretaceous nannofossils. Magnified from central part of Figure 1. **3.** Hollow interior of a perforated (planktonic?) foraminifer from the lower right quadrant of Figure 1. **4.** Enlargement of Figure 3, showing Cretaceous calcareous nannofossils. Far left and far right: *Prediscosphaera stoveri.* Center: shield of *Cribrosphaerella ehrenbergii.* **5.** Sedimentary infill of a partially dissolved calcispherulid or foraminifera chamber, showing Cretaceous nannofossils of varying preservation. **6.** Enlargement of central part of Figure 5 with recrystallized shield of *Prediscosphaera cretacea* (upper left corner), partially covered *Nephrolithus frequens* (center right), *Prediscosphaera stoveri* (far right), and various fragments of several other Late Cretaceous nannofossils.

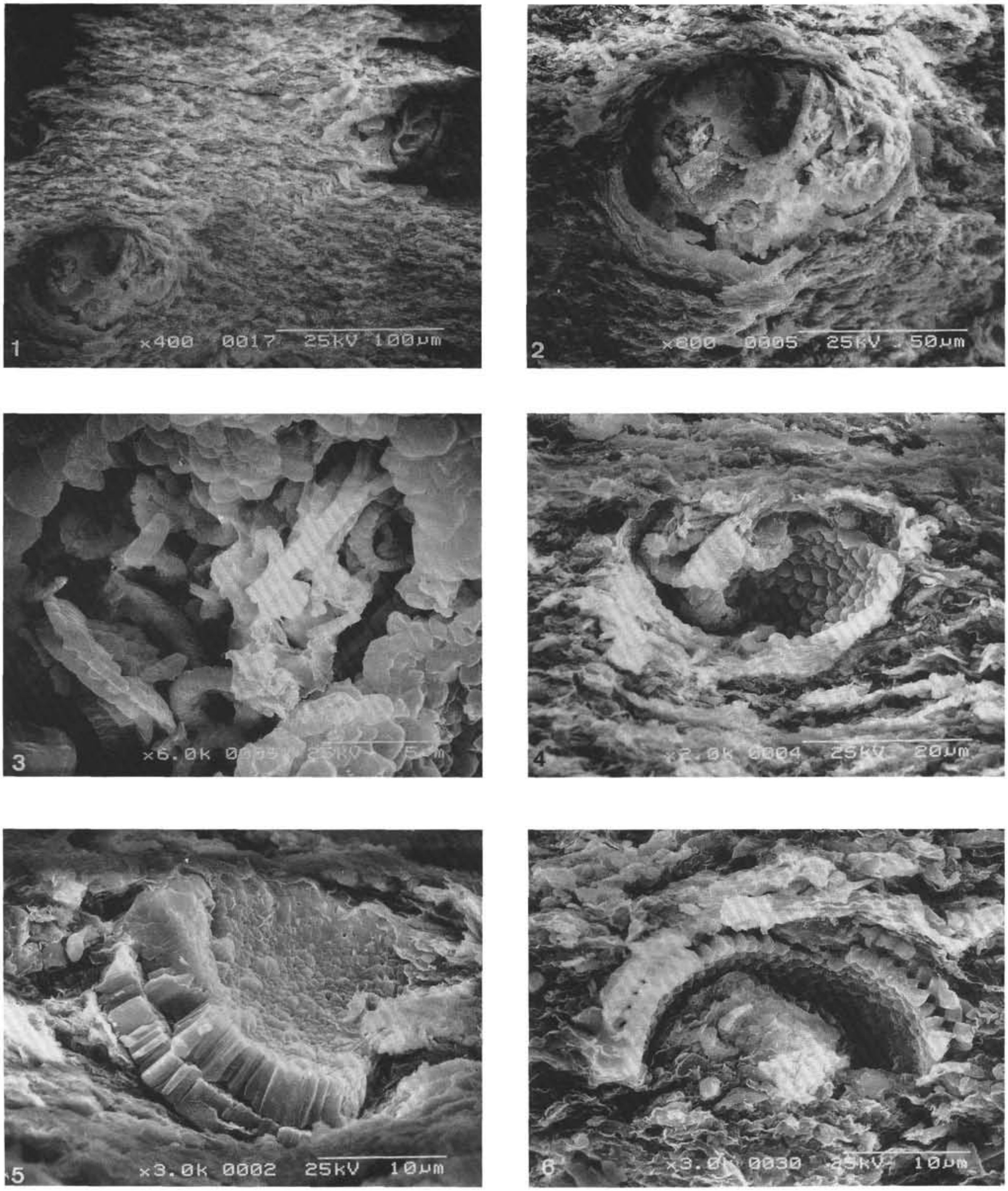

Plate 2. Cretaceous/Tertiary boundary clay (Sample 119-738C-20R-5, 96.0–96.2 cm). **1.** Sedimentary microfabric of the Cretaceous/Tertiary boundary clay with two foraminifers (lower left corner and far right margin). **2.** Foraminifers from Figure 1 (lower left corner) with interior chambers and their sedimentary fillings exposed. **3.** Slightly etched Late Cretaceous calcareous nannofossils filling an interior chamber of the foraminifer shown in Figure 2. **4.** Broken foraminifer with hollow chambers and slightly overgrown interior walls. **5.** Broken double-layered calcareous dinoflagellate cyst *(Orthopithonella* sp.). **6.** Broken calcareous dinoflagellate cyst (most likely *Orthopithonella congruenta* Fütterer (1990)).

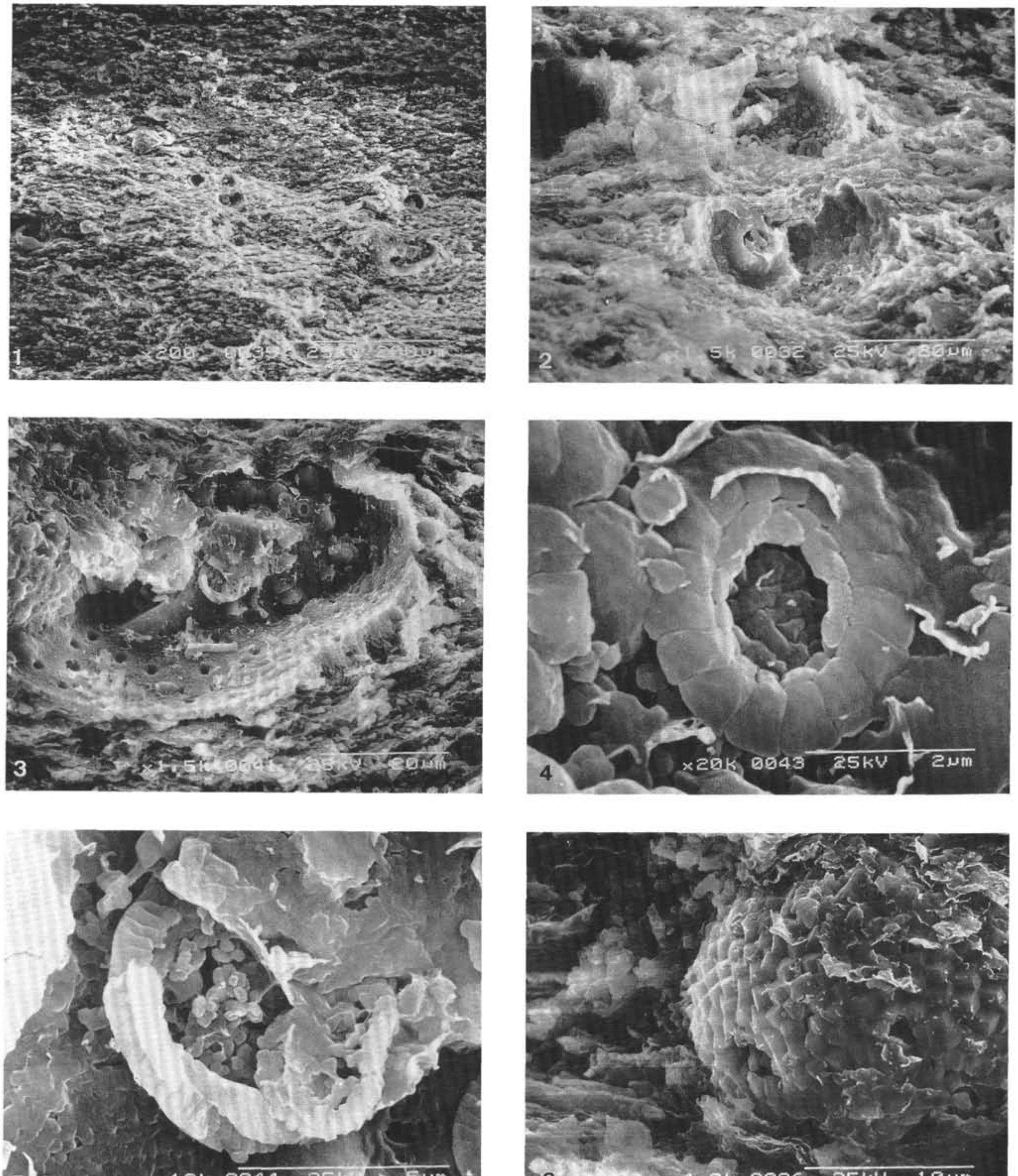

Plate 3. Cretaceous/Tertiary boundary clay (Sample 119-738C-20R-5, 96.0–96.2 cm). **1.** Sedimentary microfabric of the Cretaceous/Tertiary boundary clay with several foraminifera and calcareous dinoflagellate remains. Three areas shown in Figure 1 are progressively enlarged in Figures 2–6. **2.** Partially dissolved foraminifer (center) and calcareous dinoflagellate cyst (left upper corner) from the central area of Figure 1. **3.** Well preserved, perforated wall of a foraminifer with Upper Cretaceous nannofossils from lower right of Figure 1. **4.** Shield of *Prediscophaera cretacea* from interior of foraminifer shown in Figure 3. **5.** Shields of *Cribrosphaerella daniae* (left center) overlain by small *Nephrolithus frequens* (right center) from central part of Figure 3. **6.** Partially exposed calcareous dinoflagellate cyst *(Orthopithonella congruenta* Fütterer, 1990) from midway out on upper left diagonal in Figure 1.

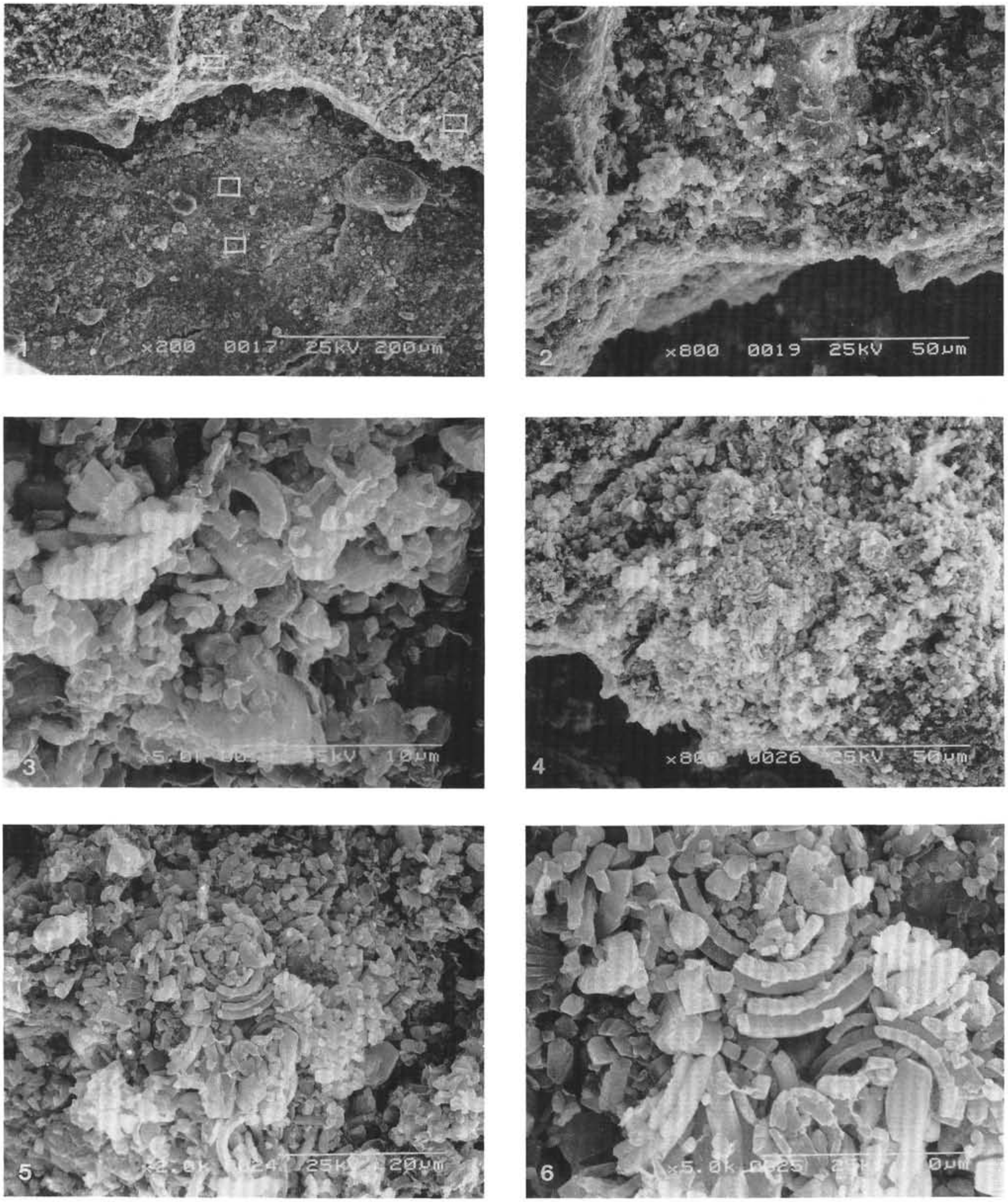

Plate 4. White ooze lamina from interval 0.5 cm above the Cretaceous/Tertiary boundary clay (Sample 119-738C-20R-5, 95–96 cm). **1.** Overview of an area showing the bedding planes of a green clay lamina (lower two-thirds of this figure) and the margin of a broken off white ooze lamina visible in the upper part of this micrograph. White rectangles indicate location of gradually magnified views leading to Figures 3 and 6 of Plate 4 and Figures 3 and 5 of Plate 5. **2.** Magnified view of central upper area of Figure 1. **3.** Microfabric showing dominance of broken nannofossil remains from central area of Figure 2 and equivalent to white rectangle in upper part of Figure 1. **4.** Magnified view of area from white ooze at right margin of Figure 1. **5.** Magnified view of central area of Figure 4. **6.** Microfabric of area corresponding to white rectangle shown at right margin of Figure 1 and to central part of Figure 5. Sediment is dominated by intact and broken shields of nannofossils and individual nannofossil elements, with minor amounts of irregularly shaped microcarbonate particles of a few microns diameter.

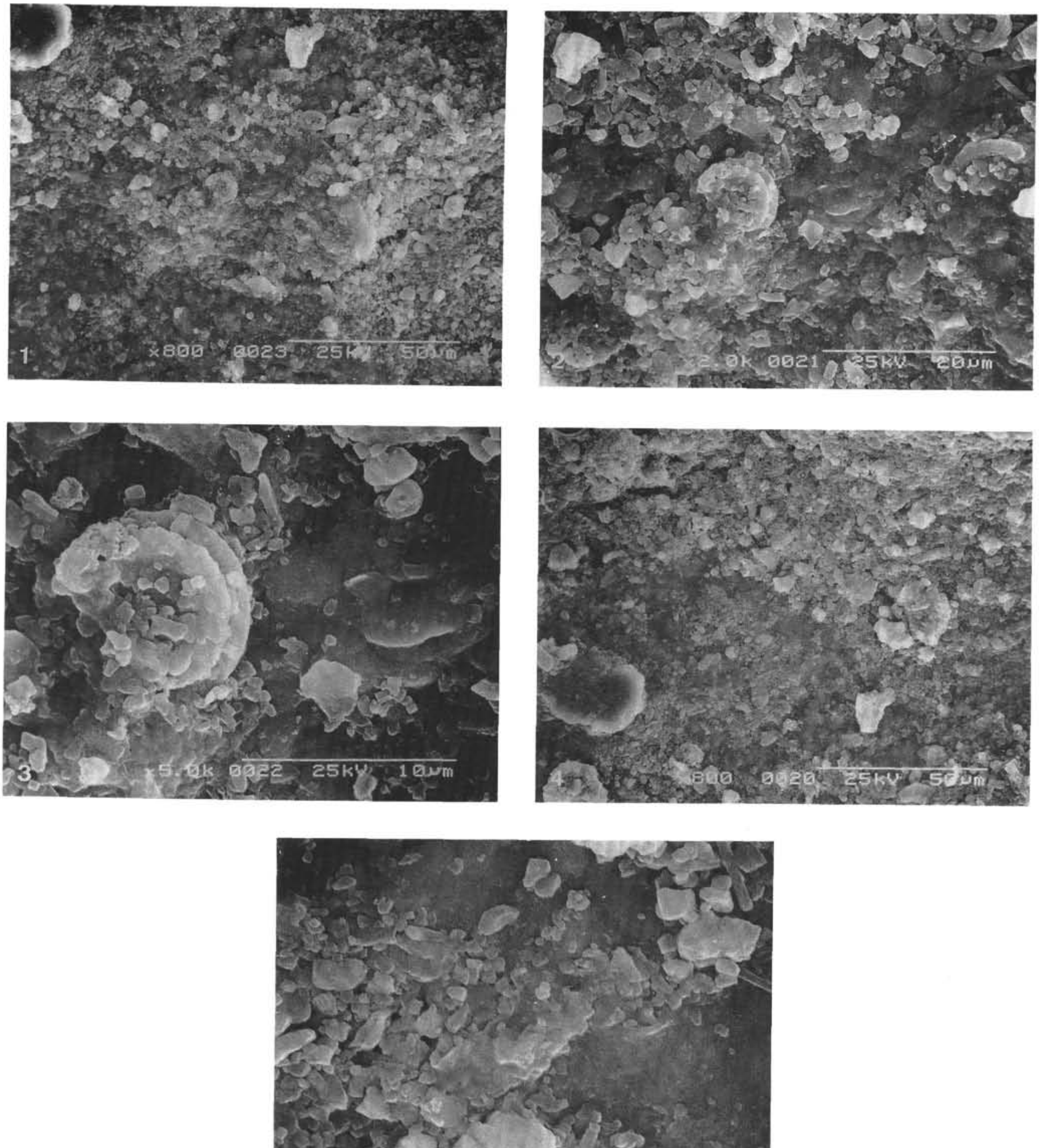

Plate 5. Green clay lamina from interval 0.5 cm above the Cretaceous/Tertiary boundary clay (Sample 119-738C-20R-5, 95–96 cm). **1.** Magnified view of clay lamina surface from lower center in Figure 1 of Plate 4. **2.** Magnified view of central area of Figure 2. **3.** Proximal view of *Markalius inversus* (circular morphotype) embedded with additional microcarbonate particles in clayey matrix. Shown area corresponds to white rectangle in lower center of Figure 1 of Plate 4. **4.** Magnified view of clay lamina surface, central area of Figure 1 of Plate 4. **5.** Magnified view of clay lamina surface with irregularly shaped microcarbonate particles partially covered by clay matrix. Area shown is that represented by white rectangle just above center of Figure 1 of Plate 4.

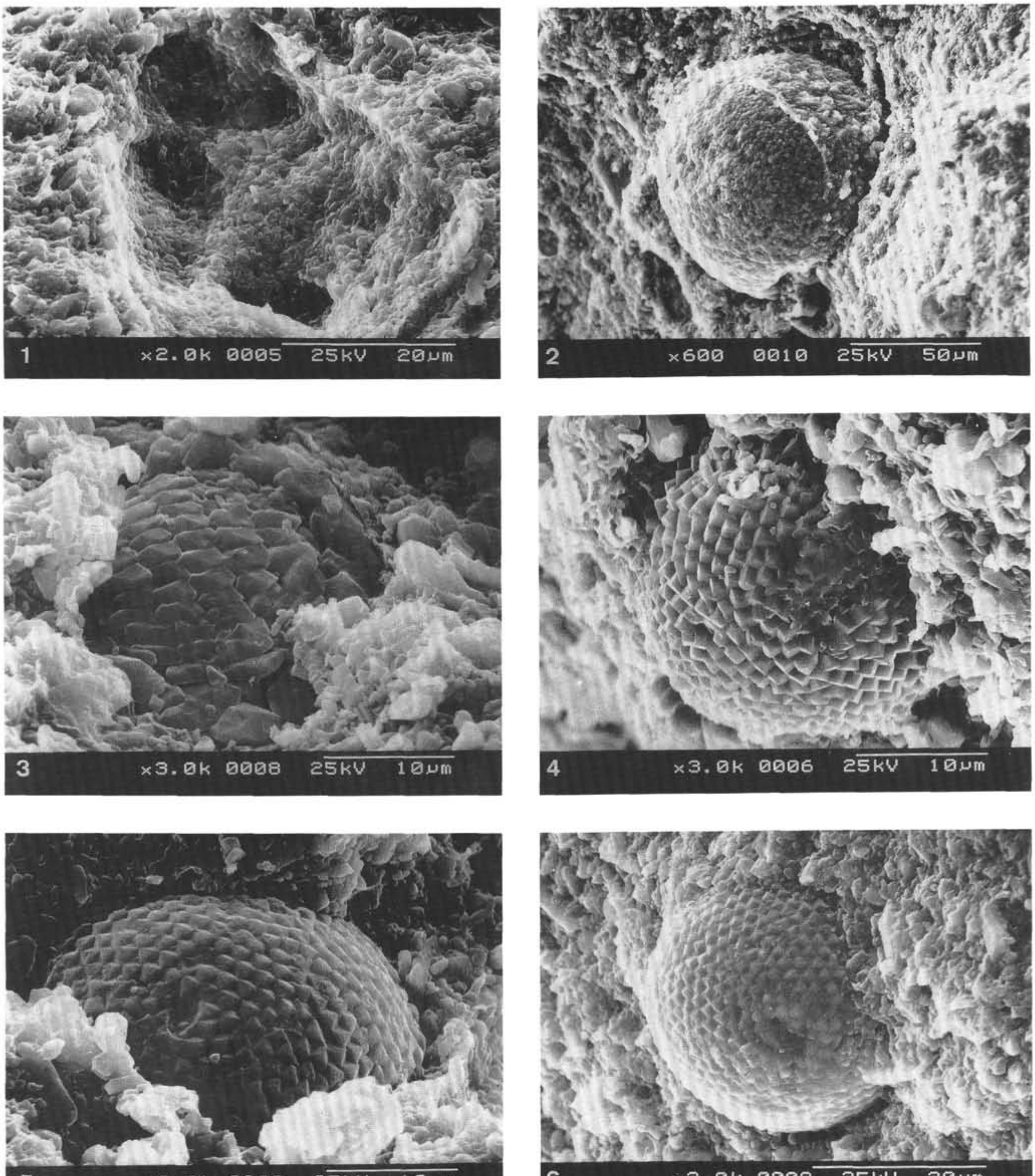

Plate 6. Layer of green clay in Sample 119-738C-20R-5, 84–85 cm, 12 cm above the Cretaceous/Tertiary boundary clay. **1.** Cast of a foraminifer in fine-grained clay-microcarbonate matrix with a few nannofossil fragments. **2.** Steinkern of a calcareous dinoflagellate cyst *(Thoracosphaera*?). **3.** Partially exposed surface of the calcareous dinoflagellate cyst *Centosphaera barbata* Wind and Wise (Wise and Wind, 1977). **4.** Partially exposed calcareous dinoflagellate cyst *Orthopithonella congruenta* Fütterer (1990) embedded in microcarbonate and clay-dominated matrix. **5.** Partially exposed calcareous dinoflagellate cyst *Orthopithonella congruenta* Fütterer (1990) embedded in microcarbonate and clay-dominated matrix. **6.** Partially exposed calcareous dinoflagellate cyst *Orthopithonella congruenta* Fütterer (1990) embedded in microcarbonate and clay-dominated matrix.